

Synthesis and Cancer Stem Cell-Based Activity of Substituted 5-Morpholino-7*H*-thieno[3,2-*b*]pyran-7-ones Designed as Next Generation PI3K Inhibitors

Guillermo A. Morales,^{*,†,§,⊥} Joseph R. Garlich,^{‡,⊥,§} Jingdong Su,[§] Xiaodong Peng,[§] Jessica Newblom,[§] Kevin Weber,[§] and Donald L. Durden^{*,||,‡}

[†]BIO5 Institute (Oro Valley), The University of Arizona, 1580 East Hanley Boulevard, Oro Valley, Arizona 85737, United States

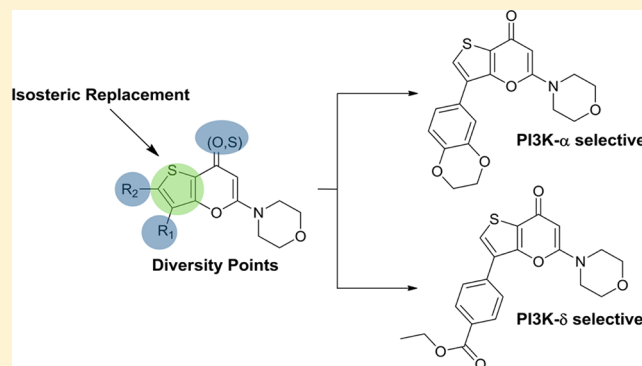
[‡]SignalRx Pharmaceuticals, 12545 El Camino Real, Suite C, San Diego, California 92130, United States

[§]Semafore Pharmaceuticals Inc., 8496 Georgetown Road, Indianapolis, Indiana 46268, United States

^{||}Department of Pediatrics, UCSD Rady Children's Hospital, Division of Pediatric Hematology–Oncology, Moores Cancer Center, UC San Diego Health System, La Jolla, California 92123, United States

Supporting Information

ABSTRACT: Dysregulation of the phosphatidylinositol-3-kinase (PI3K) pathway in a wide range of tumors has made PI3K a consensus target to inhibit as illustrated by more than 15 inhibitors now in clinical trials. Our previous work, built on the early pioneering multikinase inhibitor LY294002, resulted in the only PI3K vascular-targeted PI3K inhibitor prodrug, SF1126, which has now completed Phase I clinical trials. This inhibitor has properties that impart more in vivo activity than should be warranted by its enzymatic potency, which in general is much lower than other clinical stage PI3K inhibitors. We embarked on the exploration of scaffolds that retained such properties while simultaneously exhibiting an increased potency toward PI3K. This work resulted in the discovery of the 5-morpholino-7*H*-thieno[3,2-*b*]pyran-7-one system as the foundation of a new compound class of potential PI3K inhibitors having improved potency toward PI3K. The synthesis and cancer stem cell-based activity of these compounds are reported herein.



■ INTRODUCTION

Phosphatidylinositol 3-kinase (PI3K) is a family of intracellular enzymes that transduce signals arising from cell surface receptors such as G-protein-coupled receptors and tyrosine kinase receptors to inside of the cell. There are several classes of PI3K of which the class I PI3Ks has been the most studied and consists of the α , β , γ , and δ isoforms.¹ All of these enzymes phosphorylate the 3-position hydroxyl group of the inositol ring of phosphatidylinositol and in particular convert PIP2 (phosphatidylinositol(4,5)-bisphosphate) into PIP3 (phosphatidylinositol(3,4,5)-trisphosphate). This process is opposed by the well-studied tumor suppressor PTEN, which is a phosphatase that converts PIP3 back into PIP2. Together, PI3K and PTEN are considered the “Yin and Yang” of oncogenic signaling.² The PIP3 that is produced by PI3K in turn is a crucial activator of downstream signaling elements, of which the most important and most studied is AKT. Because of PI3K's critical role in cell functions, it is a highly desirable target to inhibit for treating cancer.³ This is best illustrated by more than 15 different PI3K inhibitors reaching phase I clinical trials.⁴ Additionally, the activation of PI3K by mutations or by aberrant signaling decreases the effects of many anticancer

treatments, so combinations of PI3K inhibitors with other drugs are being investigated in early clinical trials.⁵ PI3K inhibitors are also being investigated for the treatment of inflammatory diseases.⁶

The natural product wortmannin was discovered as the first PI3K inhibitor and was found to covalently bind to the catalytic ATP pocket of PI3K and termed an irreversible inhibitor.⁷ There was considerable toxicity associated with wortmannin, perhaps due to its irreversible binding, which may have tainted this class of compounds and set back interest for several years.⁷ The natural product quercetin was also found to be a PI3K inhibitor, but differed mechanistically from wortmannin in that it was a competitive inhibitor by competing with ATP for the kinase catalytic site of PI3K. Analogues of quercetin were synthesized and led to the first generation of designed small molecule PI3K inhibitors, of which LY294002 (**1**) (Figure 1) was found to be the most potent. An SAR study revealed that the phenyl group (8-position) and the morpholino group (2-position) on the chromenone system were crucial for PI3K

Received: October 19, 2012

Published: February 14, 2013

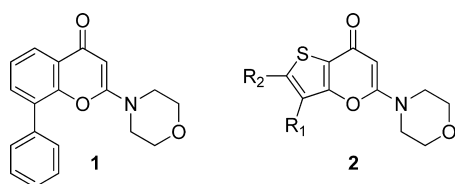


Figure 1. 2-Morpholino-4*H*-chromen-4-one (**1**) and 5-morpholino-7*H*-thieno[3,2-*b*]pyran-7-one (**2**) scaffolds.

affinity.⁸ Six years later, PI3K- γ was cocrystallized with **1**, further revealing that (1) the oxygen of the morpholine group forms a key hydrogen bond interaction with Val882 (hinge region), (2) the phenyl group (8-position) resides at a location where the ribose unit of ATP is accommodated, and (3) the carbonyl group engages into a putative hydrogen-bond interaction with Lys833.⁹ These findings led to the birth of new PI3K-targeted scaffolds where the morpholine group was used as a “warhead” to gain affinity toward PI3K’s ATP catalytic pocket.^{10,11}

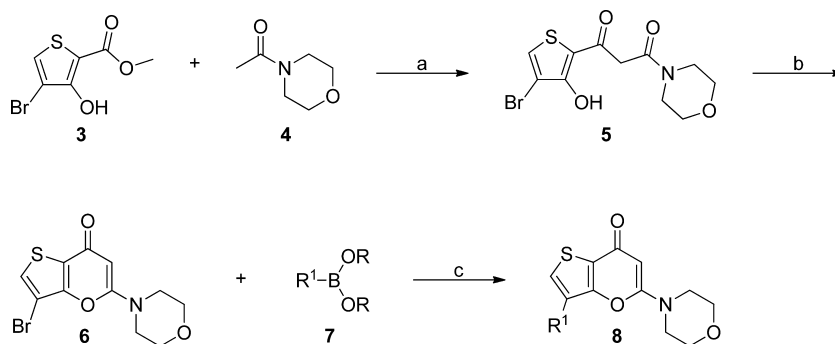
The development of PI3K-targeted therapeutics faced two paradigms, namely simultaneously inhibit all PI3K isoforms (pan inhibition) or only one (isozyme selective). PI3K pan inhibition is desirable based on the theory that if all PI3K isoforms are blocked in cells wherein this pathway is dysregulated, such an approach will effectively block the ability of tumor cells to survive, grow, and proliferate.^{12–14} A potential concern this approach faces, however, is that this could lead to unwanted toxicities. To address this potential concern, an isozyme-selective PI3K inhibition approach has been proposed as an alternate way to pharmacologically modulate the PI3K cell signaling pathway.¹⁵ Genetic alterations of PIK3CA, the gene for PI3K- α , in cells leads to PIK3CA mutations and amplifications, where PI3K- α isozyme selective inhibitors can be of therapeutic use.¹⁶ For tumors that are PTEN-deficient, it has been established that it is the PI3K- β isozyme that drives growth and survival, and for such tumors, PI3K- β selective inhibitors are expected to exhibit therapeutic benefits.¹⁷ While PI3K- α and PI3K- β are more ubiquitously expressed, PI3K- δ is primarily found in leukocytes, where its overexpression is generally exhibited in lymphoma cancers and B-cell malignancies affecting the immune system. Just like PI3K- δ , the PI3K- γ isozyme is also found mainly in leukocytes with a limited tumorigenic role and a more prominent role in inflammatory diseases.¹⁵

The pan-PI3K inhibitor **1** has served as a research tool for the past 22 years, generating an avalanche of studies cited in over 6000 publications listed on PubMed. Compound **1** suffers from poor oral availability and very fast metabolism.¹⁸ Compound **1** is a pan-class I isoform inhibitor of PI3K (α , β , γ , δ) with moderate potency.¹⁹ It has also been shown to inhibit related kinases important to cancer survival and progression such as PIM-1, PLK-1, DNA-PK, and mTOR kinase.^{20–24} Compound **1** has shown properties independent of its PI3K inhibition that may be unique among synthetic PI3K inhibitors including inducing oxidative stress²⁵ and inhibition of drug efflux mechanisms.²⁶ Despite the poor drug-like properties and modest potency, **1** has demonstrated significant anticancer activity in animal models at competitive dose levels.^{27,28} One approach to building on these unique properties has been to create prodrugs of **1**. One such compound is SF1126, a vascular targeted prodrug of **1**, shown to have improved preclinical¹² activity as well as demonstrated safety and signs of clinical efficacy in phase I trials in patients with solid tumors²⁹ and B-cell malignancies.³⁰

At the time we began the research described herein (early 2007), there were very limited examples of small molecule PI3K inhibitors beyond **1**. On the basis of the compelling medical interest in PI3K inhibitors coupled with our extensive experience with **1** and its prodrugs, we sought to create novel small molecule analogues with greater potency and improved drug-like properties while trying to maintain the desirable spectrum of kinase inhibition and unique properties such as induction of oxidative stress.

After a thorough analysis of the reported chemotypes exhibiting PI3K affinity, it was noted that a direct thiophene analogue of **1**’s chromenone core had not been explored for PI3K inhibition. The use of thiophene as a bioisostere of the phenyl ring moiety is well documented, but because the phenyl ring is a central part of the scaffold that fits within the catalytic site, it was not known how the thiophene substitution might affect the overall fit within the enzyme. Therefore, we pursued the construction and exploration of the 5-morpholino-7*H*-thieno[3,2-*b*]pyran-7-one (**2**) system as the foundation of a new compound class of potential PI3K inhibitors as anticancer agents focusing primarily on PI3K- α inhibition.

Scheme 1. Synthesis of the 5-Morpholino-7*H*-thieno[3,2-*b*]pyran-7-one Series **8**^a



^aReagents and conditions: (a) LDA, THF, 0 °C → RT; (b) Tf₂O, DCM, RT; (c) Pd(PPh₃)₄ or PdCl₂(dppf), Cs₂CO₃, DME, MW, 130 or 180 °C, 15 min.

■ SYNTHESIS

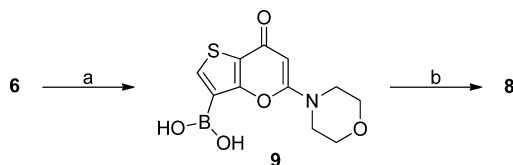
To validate scaffold **2**, we pursued the synthesis of the phenyl-containing thienopyranone **26** to compare it with its chromenone counterpart **1**.

The synthesis of the thienopyranone scaffold began with the alkylation of methyl 4-bromo-3-hydroxythiophene-2-carboxylate **3** with *N*-acetylmorpholine **4** using LDA in THF to afford 1-(4-bromo-3-hydroxythiophen-2-yl)-3-morpholinopropane-1,3-dione **5** which, upon treatment with triflic anhydride, underwent intramolecular cyclization–dehydration to afford the key intermediate 3-bromo-5-morpholino-7*H*-thieno[3,2-*b*]pyran-7-one **6**. With intermediate **6** in hand, we now have the new thienopyranone core with a bromo atom strategically placed to allow the introduction of a wide range of functionalities and substituents via halogen replacement reactions.

The first thienopyranone derivatization round began with the incorporation of diverse aromatic and heteroaromatic functionalities via microwave-assisted Suzuki carbon–carbon coupling conditions using commercially available aromatic and heteroaromatic boronic acids/esters **7** in the presence of either Pd(PPh₃)₄ or PdCl₂(dppf) in Cs₂CO₃/DME at 130 or 180 °C to produce the desired thienopyranone analogues **8** (Scheme 1).

To expand the scope of the Suzuki coupling reaction and avoid being limited by the commercial availability of boronic acids/esters, we reversed the role of intermediate **6** (electrophile) by converting it to its corresponding boronic acid analogue **9** (nucleophile). In this case, **6** was borylated by reacting it with pinacol borane in the presence of NiCl₂(dppf)/dppp and 1,3-bis(diphenylphosphino)propane at 160 °C in dioxane under microwave irradiation conditions. Further treatment with 1 M HCl afforded the desired boronic acid **9** (Scheme 2).

Scheme 2. Synthesis of Boronic Acid 9 for Reverse Suzuki Couplings^a

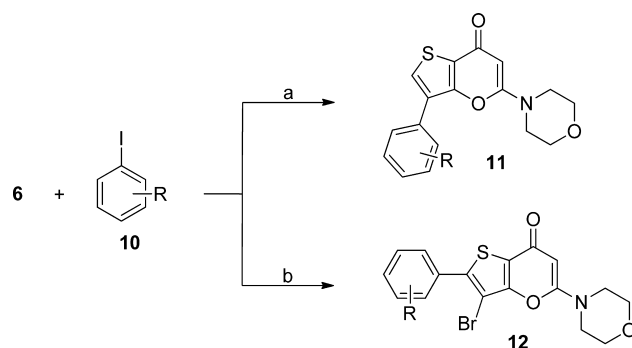


^aReagents and conditions: (a) (i) NiCl₂(dppf), dppp, 1,3-bis(diphenylphosphino)propane, pinacol borane, diisopropylethylamine, dioxane, MW, 160 °C, 15 min; (ii) aq HCl (1 M), 30 min, RT; (b) Ar–Br, Pd(PPh₃)₄, Cs₂CO₃, DME, MW, 140 °C, 15 min.

In addition to the Suzuki reaction, we were able to directly carry out aryl–aryl couplings using **6** and iodoaromatics in one pot using bis(pinacolato)diboron in the presence of PdCl₂(dppf) in Cs₂CO₃/DME at 140 °C under microwave irradiation conditions. Moreover, we were able to selectively activate the H-thiophene site carrying out a carbon–carbon (aromatic–thiophene) coupling reaction while leaving the bromo group intact. This was achieved by reacting **6** with iodobenzene using PdCl₂(PPh₃)₂ in combination with AgNO₃ and KF in DMSO at 120 °C under microwave irradiation conditions, affording **12** (Scheme 3).³¹

Another carbon–carbon coupling strategy used was the Sonogashira reaction where bromo intermediate **6** was reacted with aromatic alkynes in the presence of PdCl₂(PPh₃)₂ and CuI

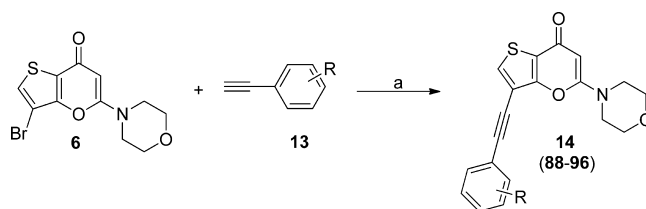
Scheme 3. Selective Thiophene Carbon–Carbon Couplings between 6 and Iodoaromatics^a



^aReagents and conditions: (a) PdCl₂(dppf), Cs₂CO₃, DME, MW, 140 °C, 15 min; (b) PdCl₂(PPh₃)₂, AgNO₃, KF, DMSO, MW, 120 °C, 15 min.

in diisopropylamine at 100 °C under microwave irradiation conditions (Scheme 4).

Scheme 4. Sonogashira Carbon–Carbon Couplings between 6 and Alkynes^a



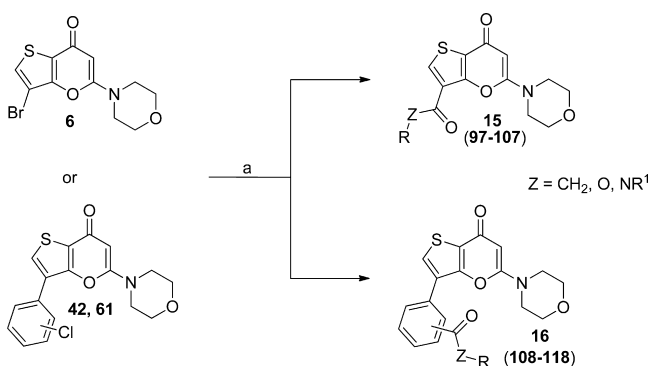
^aReagents and conditions: (a) PdCl₂(PPh₃)₂, CuI, *i*-Pr₂NH, MW, 100 °C, 20 min.

Another strategy used to create diverse analogues for SAR elucidation was the development of microwave-assisted carbonylation reactions for the one-pot synthesis of carboxylic acids, carboxylic esters, and amides. Using Mo(CO)₆ as a carbonyl source, the bromo group of **6** and the chloro group in introduced substituents were successfully replaced via a carbonyl-insertion reaction where the use of water, an alcohol, or an amine led to the formation of carboxylic acids, esters, or amides, respectively (Scheme 5). Interestingly, we were able to synthesize aromatic ketones via the Heck reaction of aromatic chlorides with butyl vinyl ether in the presence of PdCl₂(dppf) using DIPEA and DMF at 180 °C under microwave irradiation conditions (Scheme 5).^{32–34}

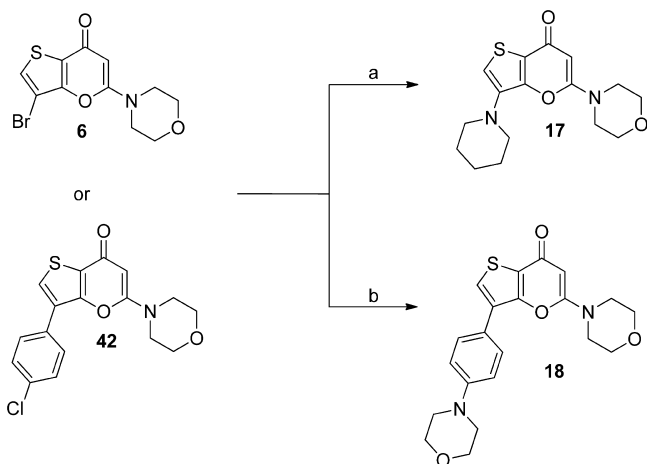
Aromatic aminations were successfully carried out via direct amine-halogen replacement (Br-thiophene, Cl-phenyl) using cyclic secondary amines, where in the case of **6**, ethyl 2-oxocyclohexanecarboxylate was used in the presence of CuI and Cs₂CO₃ in piperidine at 150 °C under microwave irradiation conditions, and in the case of chlorophenyl analogues, tBuO[−]Na⁺ was used in the presence of Pd₂(dba)₃ and XPhos in DME at 150 °C also under microwave irradiation conditions (Scheme 6).

Acylation of aniline-containing thienopyranones were carried out using acyl chlorides in pyridine at room temperature (Scheme 7).

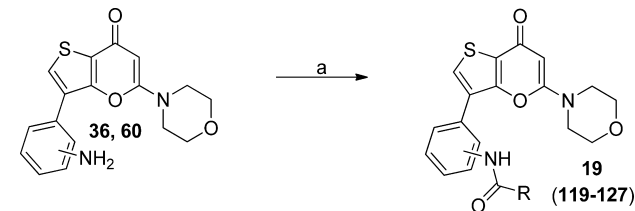
For SAR purposes, we wanted to explore the importance of the carbonyl group of the thienopyranone and chromenone systems. Transforming the carbonyl group into a thiocarbonyl

Scheme 5. Synthesis of Carboxylic Acids, Esters, Amides, And Ketones via Carbonyl Insertion and Heck Reactions^a

^aReagents and conditions: (a) For Z = O, NR¹: palladacycle, Mo(CO)₆, HO-R or HNR₁R₂, (tBu)PH⁺BF₄⁻, DBU and/or imidazole, MW, THF (125 °C, 6 min or 175 °C, 15 min) or DMSO (125 °C, 6 min). For Z = CH₂, R = H: (i) butyl vinyl ether, PdCl₂(dppf), DIPEA, DMF, MW, 180 °C, 6 min; (ii) aq HCl.

Scheme 6. Aromatic Thienopyranone Amination Reactions^a

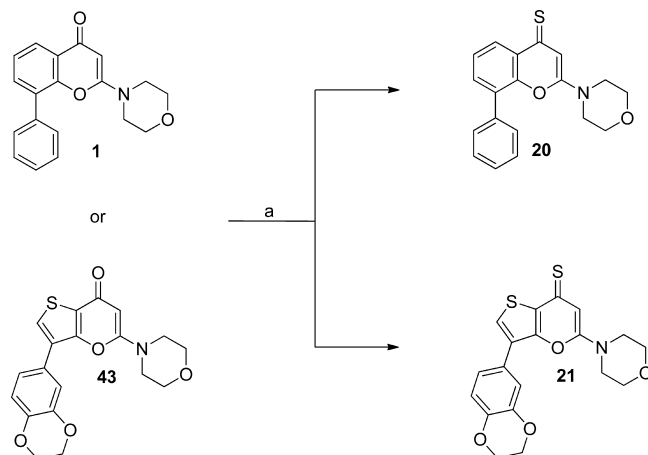
^aReagents and conditions: (a) ethyl 2-oxocyclohexanecarboxylate, CuI, Cs₂CO₃, piperidine, MW, 150 °C, 15 min; (b) tBuO⁻Na⁺, Pd₂(dba)₃, morpholine, DME, MW, 150 °C, 15 min.

Scheme 7. Acylation of Aniline-Containing Thienopyranones^a

^aReagents and conditions: (a) acyl chloride, pyridine, 0 °C → RT.

group was accomplishing by treating compounds **1** and **43** with Lawesson's reagent in toluene at 130 °C under microwave irradiation conditions, affording the desired thienopyranthione and chromenthione derivatives (Scheme 8).

To assess the influence of the nitrogen atom in the morpholine group, a tetrahydro-2H-pyran-4-yl group was incorporated in a direct analogue of **1**. For this biphenylketone, **22** was used to alkylate pyran-containing methyl ester **23** to

Scheme 8. Thienopyranthione Synthesis^a

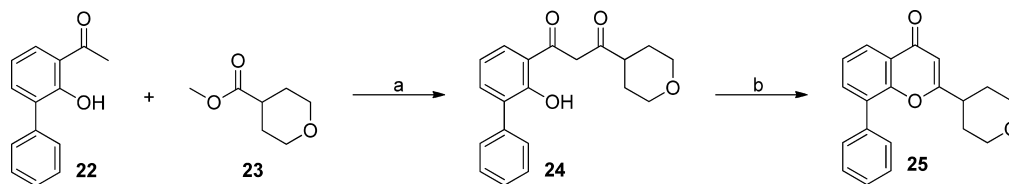
^aReagents and conditions: (a) Lawesson's reagent, toluene, MW, 130 °C, 20 min.

afford phenol-diketo intermediate **24**, which upon treatment with CuCl₂ in EtOH at 140 °C under microwave irradiation conditions afforded the desired tetrahydro-2H-pyran-4-yl analogue **25** (Scheme 9).

RESULTS AND DISCUSSION

The initial substitution of the thiophene for the phenyl core in **1** resulted in compound **26**. To our surprise, we found that compound **26** not only exhibited a similar or better PI3K and mTOR enzymatic inhibition profile than **1**, but it was also slightly more water soluble, cell permeable, and potent when tested in a cell proliferation assay using PC3 cells while downregulating the PI3K pathway as illustrated by inhibiting pAKT-S473 levels (Table 1). While compound **26** exhibited slightly increased inhibition against PI3K- α and PI3K- γ in comparison with **1**, for the PI3K- β and PI3K- δ isoforms, this compound has an increased potency of approximately 2-fold and 4-fold, respectively. Additionally, mTOR is a clinically validated target in cancer treatments and **26** demonstrated almost 2-fold improvement in inhibiting mTOR kinase activity versus **1**. Evaluation of the ability of **26** to block the PI3K pathway and decrease the pAKT activation in PC3 cells by 50% versus **1** demonstrated over a 2-fold improvement in activity. Lastly, as shown in Table 1, compound **26** showed an almost 2-fold improvement versus **1** in the inhibition of prostate cancer cell proliferation (PC3 cell line).

With the above results providing the validation of the thienopyranone core as a viable chemotype for PI3K inhibition, we synthesized 19 diverse analogues (**26–44**) to obtain an early SAR profile on the new scaffold. As we focused our efforts toward PI3K- α selective inhibition, we pursued a structure-based design approach, developing a predictive in silico molecular modeling model for PI3K- α . It has been established that the PI3K- α and PI3K- γ isozymes display a significant protein sequence homology (~35%) and kinase domain homology (~44%).³⁵ To accomplish this, we started with the available crystal structure of PI3K- γ cocrystallized with **1** (PDB code: 1E7V), used MOE (Computational Chemistry Group Inc.) to superimpose the human PI3K- α protein sequence from the Swiss Prot protein sequence database (<http://www.expasy.ch/sprot>) (UniProtKB/Swiss-Prot entry no. P42336, PK3CA - HUMAN) over the 3D coordinates of PI3K- γ removing both

Scheme 9. Tetrahydro-2H-pyran-4-yl Analogue of **1**^a

^aReagents and conditions: (a) LDA, THF, 0 °C → RT; (b) CuCl₂, EtOH, MW, 140 °C, 15 min.

Table 1. Comparison of IC₅₀ Values (nM) and Cellular Activity for **26** versus **1**

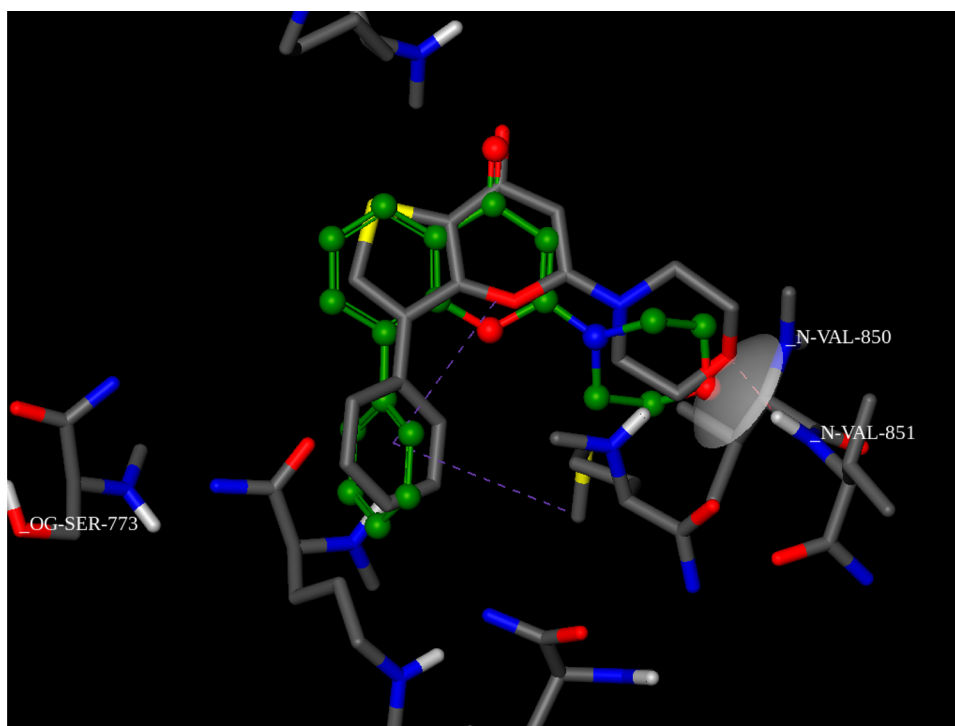
category	enzyme	1	26	fold improvement ^a
PI3K class 1A	p110- α	356	297	1.2
PI3K class 1A	p110- β	736	378	1.9
PI3K class 1A	p110- δ	3224	784	4.1
PI3K class 1B	p110- γ	1775	1570	1.1
PI3K super family enzyme	mTOR	1060	610	1.7
pathway inhibition IC ₅₀ (μ M)	pAKT	1.3	0.55	2.4
cell proliferation IC ₅₀ (nM)	PC3 cells	7500–12100	4100	1.8–3.0

^aValue for **1** divided by the value obtained for **26**.

water molecules and **1** to create a PI3K- α homology model. In our work, we use the PI3K- α numbering when referring to amino acid residues (e.g., Val882 (PI3K- γ) → Val851 (PI3K- α), Lys833 (PI3K- γ) → Lys802 (PI3K- α)). It is worth noting that as we focused on the ATP catalytic site for in silico docking, many of the residues differ between these two isoforms (e.g., PI3K- γ → PI3K- α : Thr866 → His855, Ile881 → Val850, Lys802 → Arg770, Ala805 → Ser773).³⁶

We selected a 3D grid with a 10 Å radius at the ATP binding site and proceeded to dock **1** and the 19 synthesized thienopyranone analogues (**26**–**44**) using two of the previously established pharmacophoric constraints, namely the H-bond with Val851, and the spatial location of the carbonyl group. Out of all the docking engines we tested, we found that only FlexX (BioSolveIT GmbH) could accurately dock all the thienopyranone compounds where the FlexX docking scores for the docked compounds also correlated with approximately 80% accuracy the thienopyranone analogues that exhibited PI3K- α enzymatic selectivity.

As shown in Figures 2 and 3, like in the case of **1**, new fragments introduced at the 3 position of the thienopyranone skeleton (a) are placed in the same space in PI3K that the phenyl group of **1** occupies, (b) are oriented and projected toward solvent exposure, and (c) can potentially engage in additional H-bond interactions with amino acid residues located in the outer region of PI3K's ATP catalytic site and gain PI3K binding affinity. As it is shown in Table 2, the lack of substituents at the 3 position of the thienopyranone skeleton (**33**) as well as changing the phenyl group for nonaromatic cyclic substituents (**17**, **18**) (data not shown) resulted in virtually a complete loss of affinity toward all PI3K isozymes.

Figure 2. PI3K- α homology docking model (derived from PDB code 1E7V) showing **1** and **26** superimposed.

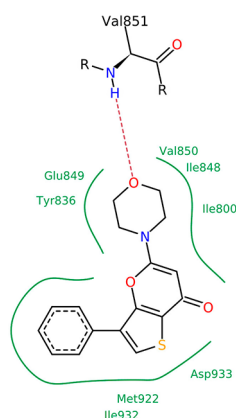


Figure 3. 2D depiction of **26** at the PI3K- α active site (derived from PDB code 1E7V).

Replacing the phenyl group with furan and thiophene groups, the latter a common phenyl isostere, gave analogues with opposite activity profiles. When the phenyl group was replaced with 2-furan (**29**), this compound exhibited almost a 3-fold improved affinity for PI3K- β while losing affinity toward the other 3 PI3K isozymes, particularly against PI3K- δ . On the other hand, when 3-furan (**42**) was introduced, activity against all PI3K isoforms was greatly reduced. An opposite trend was observed in the case of the introduction of the thiophene group, as when the phenyl group was replaced with 2-thiophene (**37**), loss in activity for all PI3K isoforms was observed. However, when 3-thiophene (**41**) was introduced, an unexpected 3-fold activity and selectivity toward PI3K- α was observed.

When 3-pyridyl (**27**) and 4-pyridyl (**28**) were used instead of the phenyl group, the former analogue retained similar PI3K- α affinity like **26** while the latter analogue exhibited a 3-fold affinity toward PI3K- α , yet both still exhibit PI3K- α selectivity. Interestingly, when 2-indolyl (**35**) was used to replace the phenyl ring of **26**, an almost 4-fold improvement in PI3K- α affinity was found, although a 5-fold affinity increase toward PI3K- γ was also observed. On the other hand, when the indolyl moiety was connected to main scaffold at indolyl's 5 position (**40**), pan-PI3K inhibition was achieved (161–667 nM range) with slight preference for PI3K- α and PI3K- β .

During our early SAR assessment, a common trend was found where analogues containing electron donating groups on the phenyl ring of **26** (with the exception of 3-amino analogue **34**) all exhibited higher affinity toward all 4 PI3K isozymes and, particularly, PI3K- α selectivity (compounds **30**, **31**, **32**, **34**, **38**, **39**, **43**, **44**). Of particular note was compound **43**, as it was the first compound of the series to exhibit selective PI3K- α inhibition (IC_{50} = 34 nM) along with some of the most potent inhibition of the other isoforms, defining it as a much more potent pan-PI3K inhibitor than **1**. The PI3K- α computational docking model indicates that **43** is expected to engage an additional H-bond interaction with Thr856 which explains the high potency of this analogue (Figure 4).

One unforeseen discovery was when the 4-*N*-methylamino analogue **55** was tested and compared against its 4-*N,N*-dimethylamino relative **32**, the latter dimethylated aniline analogue exhibited PI3K- α selectivity with an IC_{50} value of 95 nM, while the former monomethylated analogue exhibited both PI3K- α and PI3K- δ selectivity (IC_{50} = 56 and 26 nM, respectively).

To assess the impact of inserting aliphatic groups between the phenyl group and the thienopyranone core in **26**, two analogues containing a *para*-methoxyphenyl group with a methylene (**45**) and alkynyl (**92**) linker were made and found that, in the case of **45**, a 3-fold loss against PI3K- δ was observed while exhibiting almost a 2-fold increase in potency against PI3K- α and PI3K- β , and in the case of **92**, activity against PI3K- α was practically the same, with a dramatic loss against PI3K- δ affinity (note: PI3K- β data not available).

Electron withdrawing groups were introduced at the *para* position of the phenyl ring in **26**, whereupon it was observed that inclusion of a nitrile group (**46**) was detrimental for PI3K- α affinity (IC_{50} = 4.6 μ M) followed by a trifluoromethyl group (**49**) (IC_{50} = 551 nM). However, in the case of Cl (**47**) and carboxylic acid (**69**), the affinity toward PI3K- α increased (IC_{50} = 112 and 80 nM, respectively).

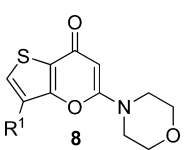
The PI3K- α model suggests that when **26** is accommodated at the ATP binding site, substituents at the 3 and 4 positions on the phenyl ring can be tolerated, particularly position 4, as substituents are projected toward solvent exposure. To probe the extended space from the ATP pocket while searching for additional interactions, we synthesized 3- and 4-substituted amide analogues containing a pyridyl moiety and found that all analogues (**110**, **111**, **113**, **115**, **117**) exhibited higher potency against PI3K- α compared to **26** where the trend was that the 3-substituted amides (**115**, **117**) were more potent than the 4-substituted ones (**110**, **111**, **113**).

We then proceeded to explore the PI3K inhibition profile of several reverse-amide analogues and discovered that while the 3-substituted reverse amide analogues (**124**, **125**) suffered a great loss of PI3K- α affinity (IC_{50} = 24 μ M and 14 μ M, respectively), the 4-substituted reverse amide analogues (**119**, **126**) were quite active, with compound **126** being the most potent PI3K- α analogue made in this series (IC_{50} = 14 nM). A molecular docking analysis of compound **126** indicates that, in addition to the required H-bond interaction with Val851, the phenyl group engages in four hydrophobic interactions with Met772, Trp780, Ile800, and Met992, while the pyridyl group forms two hydrophobic π -stacking interactions with Trp780 and His855 (Figure 5). We rationalize that the high PI3K- α affinity exhibited by **126** can be attributed to the combination of all these interactions at the catalytic site.

To investigate the impact of the carbonyl group of the chromenone scaffold, **1** was treated with Lawesson's reagent under microwave irradiation conditions and converted into the corresponding thione **20** and found to lose PI3K affinity against all isoforms (Figure 6). This observation was confirmed with the synthesis of **21**, which also exhibited loss of PI3K enzymatic affinity (data not shown).

Moreover, to also assess the role of the amino group within the morpholino moiety in **1**, compound **25** was made where a tetrahydro pyranyl group was present. This change was found to be detrimental for PI3K- α activity, as only a 44% inhibition at 10 μ M was detected.

Although we focused our efforts on PI3K- α inhibition, this compound series afforded three PI3K- δ selective analogues, namely **51**, **57**, and **58** (see Table 3). The most clinically advanced δ -isoform selective PI3K inhibitor CAL-101 (**128**) (recently renamed GS-1101)³⁷ is included in Table 3 for comparison. A comparison of δ selectivity is shown in Table 4 and demonstrates better selectivity against the γ isoform than **128** for all three compounds but less selectivity against α and β isoforms.

Table 2. Pan-PI3K Inhibition Profile of 5-Morpholino-7H-thieno[3,2-*b*]pyran-7-one Analogues (IC₅₀ Values in nM)


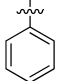
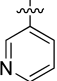
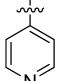
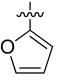
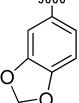
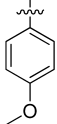
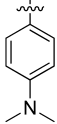
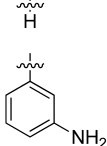
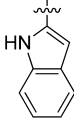
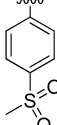
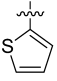
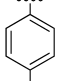
Compound	R ¹	PI3K- α	PI3K- β	PI3K- δ	PI3K- γ
26		297	378	784	1570
27		294	1027	>50000	8780
28		682	2554	>23000	5460
29		556	134	>30000	4220
30		75	367	481	385
31		61	310	555	553
32		95	693	190	211
33	H	7158	9247	>50000	>50000
34		154	NA	9807	6300
35		77	2757	8936	314
36		4539	5241	13830	7500
37		699	1205	>23000	5200
38		238	>50000	1142	1390

Table 2. continued

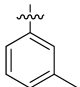
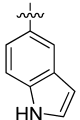
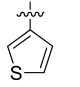
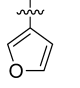
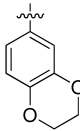
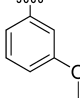
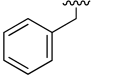
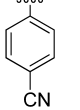
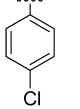
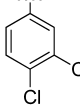
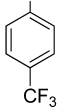
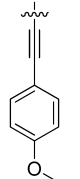
Compound	R ¹	PI3K- α	PI3K- β	PI3K- δ	PI3K- γ
39		116	175	3998	2140
40		217	161	649	667
41		110	568	>20000	4990
42		1857	7047	>50000	9180
43		34	214	960	158
44		72	371	7894	1310
45		176	150	2420	1090
46		4598	>50000	>50000	>50000
47		112	418	3732	2310
48		100	139	278	586
49		551	632	4200	5560
92		242	NA	>50000	808

Table 2. continued

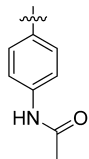
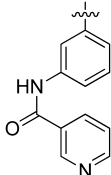
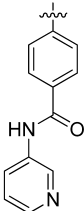
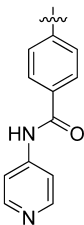
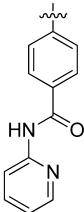
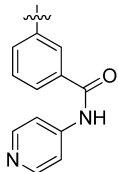
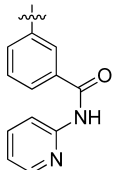
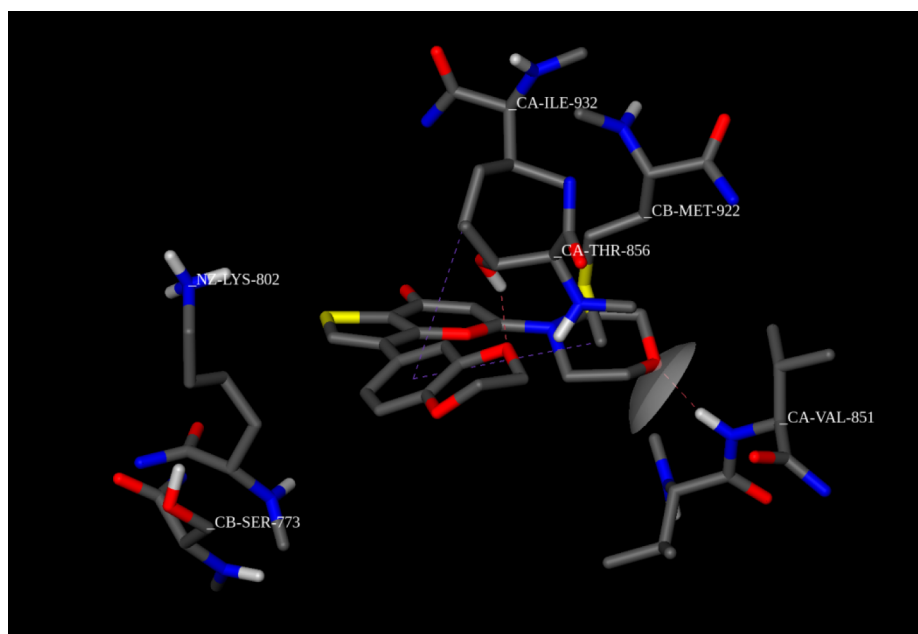
Compound	R ¹	PI3K- α	PI3K- β	PI3K- δ	PI3K- γ
123		85	8930	125	503
55		56	195	26	441
119		53	244	20	410
69		80	240	NA	NA
124		24000	NA	NA	NA
125		14000	NA	NA	NA
126		14	NA	NA	NA
110		109	NA	NA	NA

Table 2. continued

Compound	R ¹	PI3K- α	PI3K- β	PI3K- δ	PI3K- γ
111		187	NA	NA	NA
113		86	NA	NA	NA
115		71	NA	NA	NA
117		66	NA	NA	NA

Figure 4. PI3K- α homology docking model (derived from PDB code 1E7V) of compound 43.

Although it is not clear why these analogues exhibit such great affinity toward PI3K- δ , it should not be a surprise that **51** and **57** exhibit similar PI3K inhibition profile as they only differ from each other by one methylene unit on the ester component. On the other hand, compound **58** is structurally

distinct, having a pyrimidine group instead of the phenyl group as well as having a *N*-methyl-piperazine moiety whose sp^3 -based *N*-methyl group is prone to act as a hydrogen-bond acceptor potentially, establishing a yet-to-be-determined additional key interaction resulting in the observed acute PI3K- δ affinity.

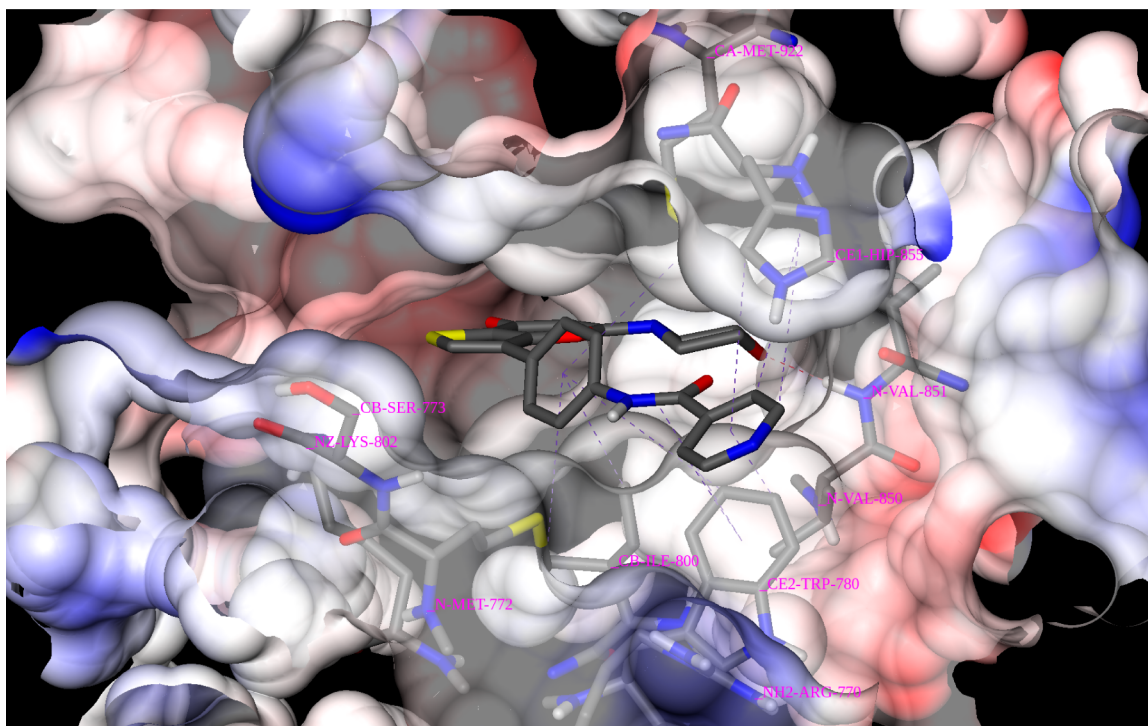


Figure 5. Binding mode of **126** docked in the catalytic site of the PI3K- α homology model (derived from PDB code 1E7V). Coloring of surface area based on formal charges (blue = positive, red = negative, white = neutral).

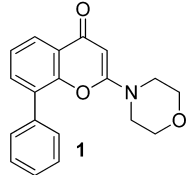
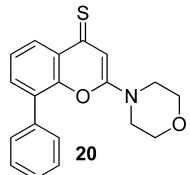
	IC ₅₀ (nM)			
	PI3K- α	PI3K- β	PI3K- δ	PI3K- γ
 1	356	736	3223	1775
 20	1006	1161	14940	3945

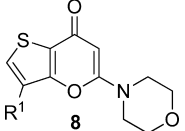
Figure 6. PI3K profile of **1** and its thione analogue **20**.

Biochemical Analysis of Potency of Compounds. To ascertain the relative potency of the different thienopyranone derivatives in cell-based assays, we turned to several PI3K activated human tumor cell lines, PC3, H1299, and 786-O.

The inhibition of the PI3K pathway by compounds **43** (pan-PI3K inhibitor) and **51** (δ -PI3K selective) was demonstrated in PC3 (prostate cancer) cells by the decreased phosphorylation of the key pathway element AKT (pAKT) as shown in Table 5. These data show potent pathway inhibition for both compounds at basal levels with no stimulation (PBS) or with the growth factor stimulation by VEGF or Bv8 (*Bombina variegata* peptide 8). Bv8 stimulation of angiogenesis is thought to be a resistance mechanism that bypasses VEGF and thus induce tumors to be refractory to anti-VEGF therapies.^{38,39} Thus, inhibition of angiogenic stimulation via this mechanism (blocking Bv8 signaling through AKT) might represent a new approach to inhibit VEGF-resistant angiogenesis and is accomplished by both the pan and δ selective inhibition of

PI3K. Also, potent inhibition of AKT activation under insulin-like growth factor (IGF) stimulation conditions was noted. In all cases, the pan-inhibitor **43** showed more potency than the δ -selective compound **51**. Inhibition of cellular proliferation by the pan-PI3K inhibitors **32** and **43** versus **1** is shown in Table 6. These results demonstrate the dramatic increase in potency across prostate (PC3), lung (H1299), renal cell (786-O), and breast cancer (BT-474) cell lines for compounds with the new thienopyranone scaffold versus **1**.

Cancer Stem Cell Inhibitory Activity. Considerable evidence implicates PTEN, PI3K, and the GSK3 β / β -catenin pathway in the control of breast cancer stem cell proliferation and expansion.^{40,41} Hence, we tested our PI3K inhibitors for the capacity to block a well-studied putative cancer stem cell phenotype, adhesion independent growth of mammospheres in MCF7 cells. The evaluation of two pan-PI3K inhibiting compounds (**43** and **119**) for their ability to inhibit breast cancer mammosphere formation is shown in Figure 7. SF1126,

Table 3. PI3K- δ Selective Inhibitors (IC₅₀ Values in nM) Including 128 (CAL-101)


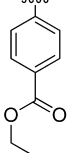
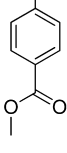
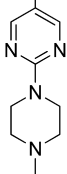
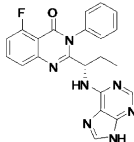
Compound	R ¹	PI3K- α	PI3K- β	PI3K- δ	PI3K- γ
51		714	1750	27	1170
57		400	3600	12	547
58		345	433	18	1080
128		820	562	2.5	89

Table 4. Comparison of New Compounds with 128 for δ Selectivity

compd	isoform selectivity multiples of PI3K- δ versus ^a		
	PI3K- α	PI3K- β	PI3K- γ
51	26	65	43
57	33	300	45
58	19	24	60
128	328	225	36

^aDivide PI3K-isoform IC₅₀ by the IC₅₀ for PI3K- δ isoformTable 5. Concentrations (μ M) of Compounds 43 and 51 Required to Inhibit pAKT to Half-Maximal Levels Stimulated by Bv8, VEGF, and IGF in PC3 (Prostate Cancer) Cell Line as Described in the Experimental Section

stimulant	43	51
PBS	0.229	0.564
Bv8	0.1164	0.9406
VEGF	0.1523	0.3317
IGF	0.888	2.117

Table 6. Cancer Cell Proliferation IC₅₀ (μ M)

	PC3	H1299	RCC 786-O	BT-474
1	12.1	11.1	18.1	20.7
32	2.0	3.0	7.2	4.3
43	1.6	0.9	3.3	3.8

the clinical stage prodrug of 1, was included and found to be inferior to the new thienopyranone compounds in the inhibition of mammosphere related growth in vitro. The approved anticancer kinase inhibitor lapatinib was also included as an internal control. We evaluated each compound at 1 and 10 μ M concentrations. These results show that the new compounds are statistically more potent toward cancer stem cells than lapatinib, the EGFR (ErbB2 and ErbB1) kinase inhibitor shown clinically to decrease breast cancer stem cells in biopsies.⁴² The treatment of MCF7 mammosphere cultures with different inhibitors in vitro resulted in the following results: SF1126 (10 μ M), 36% of control; Lapatinib (1 μ M), 67% of control; compd 43 (10 μ M), 12.4% of control; compd 43 (1 μ M), 39.9% of control; compd 119 (10 μ M), 13.7% of control, and compound 119 (1 μ M), 41.2% of control. The thienopyranone compounds 43 and 119 were noted to be 2-fold more potent compared to lapatinib in blocking mammosphere formation at equimolar concentrations in vitro.

In summary, we have successfully identified and made a thiophene isostere of the well-known chromenone system found in 1. This new 5-morpholino-7H-thieno[3,2-b]pyran-7-one compound series afforded analogues with PI3K- α selectivity as predicted by our PI3K- α homology model. Additionally, in some cases, analogues displayed an unexpected affinity toward other PI3K isozymes, such as compounds 51, 57, and 58 (PI3K- δ selectivity). Cell-based assays demonstrated that these compounds potently inhibit the downstream target of PI3K, pAKT, confirming their inhibitory modulation of the PI3K cell signaling cascade. Also, cell-based assays demon-

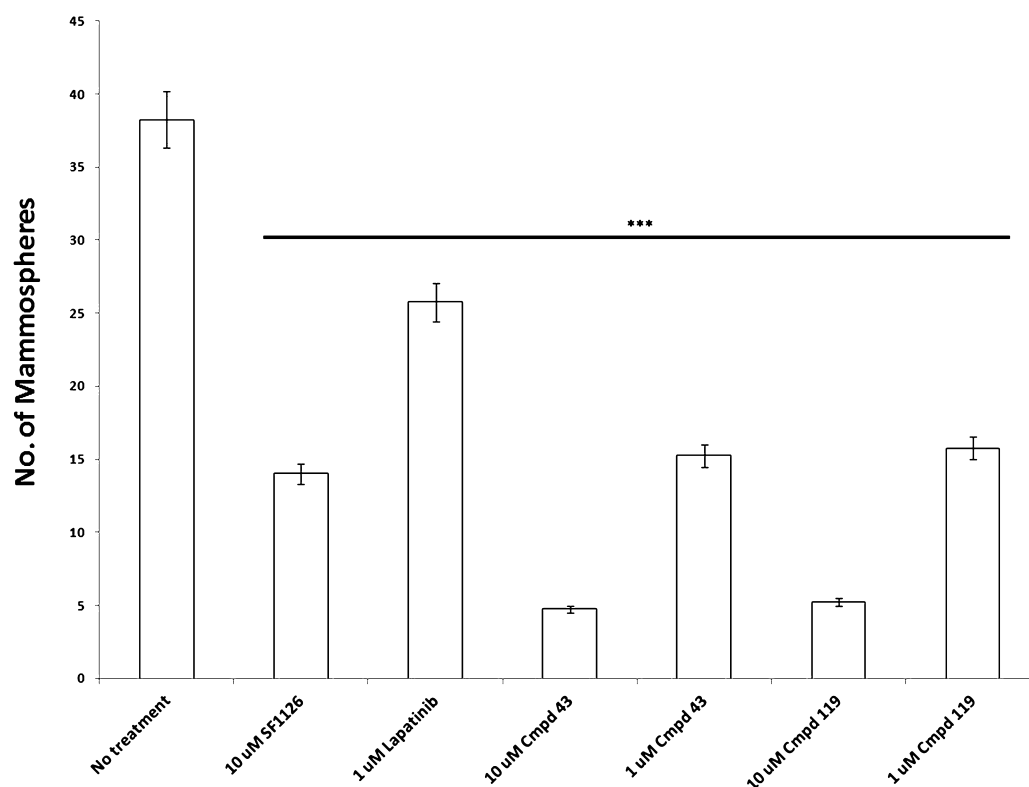


Figure 7. Breast cancer mammosphere assay: The number of mammospheres formed from MCF7 cells plated in treated 96-well plates is plotted on Y-axis versus treatment on X-axis. As indicated by the horizontal bar, all treated groups were significantly decreased relative to control untreated cells $p < 0.001$. Other statistical comparisons included: SF1126 (10 μM) to compound **43** (10 μM), $p = 3.3 \times 10^{-5}$; compound **43** (1 μM) to Lapatinib (1 μM), $p = 0.00022$; compound **43** (1 μM) to SF1126 (10 μM), $p = 0.19948$; compound **43** (10 μM) to Lapatinib (1 μM), $p = 8.10 \times 10^{-7}$.

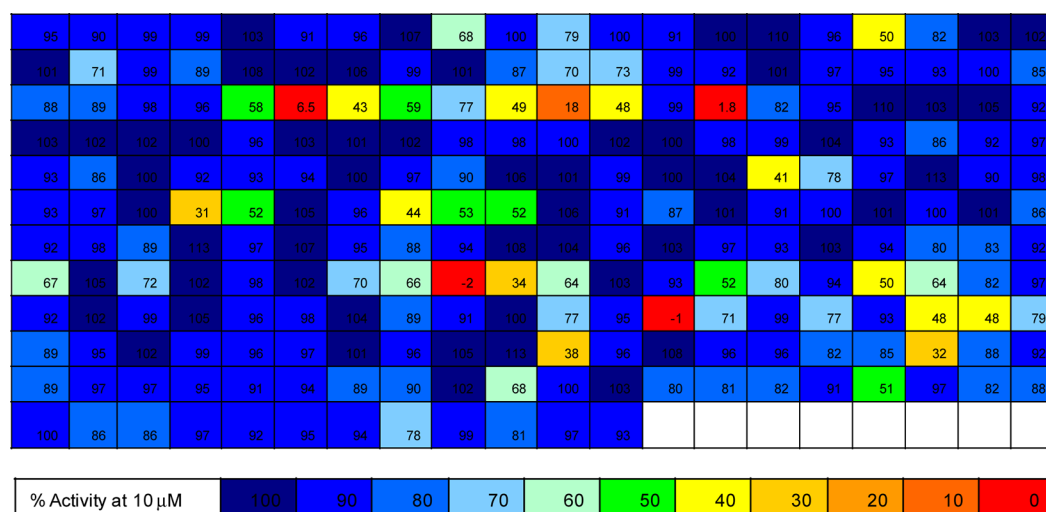


Figure 8. Kinase selectivity panel of **43** (232 kinases offered and screened by Reaction Biology Corp). Colors indicate % activity remaining testing at 10 μM going from complete inhibition (red) to no inhibition (blue).

strated potent cell growth inhibitory activity for these novel compounds. Moreover, we present evidence that PI3K inhibitors can potentially inhibit MCF7 cancer stem cell proliferation in an in vitro model. In other studies, we have confirmed the kinome specificity of compound **43** in a panel of 232 kinases (single dose at 10 μM), finding that only three other kinases are almost completely or completely inhibited: mTOR ($\text{IC}_{50} = 280 \text{ nM}$), PIM-1 ($\text{IC}_{50} = 43 \text{ nM}$), and DNA-PK ($\text{IC}_{50} = 9 \text{ nM}$) (Figure 8, red). Incidentally, besides PIM-1, the

kinase profile of **43** is similar to Novartis' clinical stage PI3K inhibitor BEZ235, which also inhibits PI3K, mTOR, and DNA-PK.^{43,44}

Additionally, we have demonstrated favorable PK and in vivo efficacy of compound **43** in mouse xenograft tumor models and performed initial PK determinations (results to be published elsewhere).^{45,46} The exploration of this new compound series is under development to optimize the current hits for PI3K pan and isoform-selective inhibition and in vivo drug like activity.

■ EXPERIMENTAL SECTION

Chemistry. All solvents and reagents were used as obtained. ^1H NMR spectra were recorded on a JEOL ECX 400 NMR spectrometer and referenced to tetramethylsilane. Chemical shifts are expressed as δ units using tetramethylsilane as internal standard (in NMR description: s, singlet; d, doublet; t, triplet; q, quartet; m, multiplet; br, broad signal; J, joules; Hz, hertz). Microwave irradiation synthesis was carried out using a Biotage Initiator 60 microwave synthesizer. Analytical data: UV absorbance (254 and 214 nm), evaporative light scattering (Alltech ELSD 2000), and mass spectra were measured with a Shimadzu LCMS-2010 spectrometer using an ESI source coupled to a Shimadzu HPLC-2010 system operating in reverse mode with a YMC CombiScreen ODS-AQ column with a particle size of 5 μm , a pore size of 12 nm, 50 mm long with a 4.6 mm I.D., using solvent A (water with 0.1% TFA), solvent B (acetonitrile with 0.1% TFA), and a flow rate of 3 mL/min starting with a mixture of 95% A and 5% B. Solvent B is linearly ramped to 95% at 5.0 min, held at 95% until 6.0 min, then linearly ramped back down to 5% at 6.5 min. Compound purification: Pure desired products were isolated from crude mixtures using the Shimadzu HPLC-MS 2010 system in preparative mode. The preparative column is a YMC CombiPrep ODS-AQ₂ with a particle size of 5 μm and a pore size of 12 nm, 50 mm long and 20 mm I.D. A flow rate of 25 mL/min starting with a mixture of 95% A and 5% B. Solvent B is linearly ramped to 95% at 25.0 min, held at 95% until 30.0 min, then linearly ramped back down to 5% at 2 min. An MRA (Rheodyne mass rate attenuator) splitter was employed to split a small part of the eluant stream, typically 0.1%, to the detectors, while the rest was sent to the Gilson 215 liquid handler. A Shimadzu LC-10ADvp pump was used to pump 3 mL/min of methanol through the MRA to deliver the sample to the UV-vis, ELS, and MS detectors. The system was run in mass-triggered mode to collect fractions containing desired product based on molecular mass. Purity of all biologically evaluated compounds was greater than 95%.

1-(4-Bromo-3-hydroxythiophen-2-yl)-3-morpholinopropane-1,3-dione (5). An oven-dried 100 mL round-bottom flask was charged with a magnetic stirring bar, tetrahydrofuran (5 mL), and lithium diisopropylamide (2.0 M in hexanes, 6.7 mL, 13.5 mmol). The reaction mixture was magnetically stirred and cooled to 0 °C under argon gas. A solution of *N*-acetylmorpholine (6.75 mmol) in tetrahydrofuran (1 mL) was added, and the reaction was stirred at 0 °C for 1 h. A solution of methyl 4-bromo-3-hydroxythiophene-2-carboxylate (4.22 mmol) in tetrahydrofuran (2 mL) was added dropwise over 5 min, and the reaction was allowed to warm to room temperature overnight. The reaction was quenched by adding aqueous 10% HCl (20 mL). The resulting solution was transferred to a separatory funnel, diluted with water (80 mL), and extracted three times with dichloromethane (100 mL). The organic layers were combined, dried over magnesium sulfate, filtered, and concentrated in vacuo to give desired product as a brown solid, and it was used without further purification.

3-Bromo-5-morpholino-7H-thieno[3,2-*b*]pyran-7-one (6). An oven-dried 100 mL round-bottom flask was charged with a magnetic stirring bar, **5** (1.95g, 5.83 mmol) and dissolved in dichloromethane (30 mL) under magnetic stirring. Trifluoromethanesulfonic anhydride (2.45 mL, 14.6 mmol) was added portionwise over 2 min, and the reaction was stirred at room temperature. After stirring overnight, the reaction was concentrated in vacuo and redissolved in methanol (10 mL). After stirring for 4 h, the reaction was concentrated in vacuo and diluted with aqueous 5% sodium bicarbonate solution (100 mL). The reaction was transferred to a separatory funnel and extracted three times with dichloromethane (100 mL). The organic layers were combined, dried over magnesium sulfate, filtered, and concentrated in vacuo to afford **6** as a brown solid (1.52g, 4.81 mmol, 82%). MS (ESI): m/z ($M + H$)⁺ 316.

5-Morpholino-7-oxo-7H-thieno[3,2-*b*]pyran-3-ylboronic Acid (9). A 20 mL microwave vial was charged with a magnetic stirring bar, compound **6** (1.20 g, 3.80 mmol), 1,3-bis(diphenylphosphino)propane (156 mg, 0.38 mmol), 1,3-bis(diphenylphosphino)propane nickel(II) chloride (205 mg, 0.38 mmol), dioxane (8 mL), diisopropylethylamine (1.98 mL, 11.39 mmol), and 4,4,5,5-tetrameth-

yl-1,3,2-dioxaborolane (1.10 mL, 7.59 mmol). The reaction mixture was magnetically stirred and heated via microwave irradiation for 15 min at 160 °C. Upon cooling to room temperature, the reaction was transferred to a separatory funnel, diluted with dichloromethane (100 mL), and washed three times with saturated aqueous ammonium chloride solution (100 mL). The dichloromethane layer was dried over magnesium sulfate, filtered, and concentrated in vacuo. The resulting brown foam was stirred in aqueous hydrochloric acid (1.0M, 100 mL) for 30 min, frozen, and lyophilized to give 5-morpholino-7-oxo-7H-thieno[3,2-*b*]pyran-3-ylboronic acid (**9**) (1.51 g, 4.15 mmol) as a brown solid. MS (ESI): m/z ($M + H$)⁺ 283.

2-Morpholinoethyl 4-(5-morpholino-7-oxo-7H-thieno[3,2-*b*]pyran-3-yl)benzoate (11). A 2 mL microwave vial was charged with a magnetic stirring bar, compound **10** (90 mg, 249 μmol), compound **6** (79 mg, 249 μmol), bis(pinacolato)diboron (70 mg, 274 μmol), cesium carbonate (325 mg, 997 μmol), dichloro[1,1'-bis(diphenylphosphino)ferrocene]palladium(II) dichloromethane adduct (6 mg, 7 μmol), and 1,2-dimethoxyethane (1 mL). The reaction mixture was sealed, and the reaction mixture was magnetically stirred and heated under microwave irradiation at 140 °C for 15 min to give desired product **11**. MS (ESI): m/z ($M + H$)⁺ 471.

3-Bromo-5-morpholino-2-phenyl-7H-thieno[3,2-*b*]pyran-7-one (12). A 2 mL conical microwave vial was charged with a magnetic stirring bar, compound **6** (50 mg, 158 μmol), phenyl iodide (27 mg, 132 μmol), potassium fluoride (11.5 mg, 198 μmol), silver nitrate (34 mg, 198 μmol), anhydrous dimethyl sulfoxide (1 mL), and dichlorobis(triphenylphosphine)palladium(II) (4.6 mg, 6.6 μmol). The reaction mixture was sealed, and the reaction mixture was magnetically stirred and heated under microwave irradiation at 120 °C for 15 min to give desired product **12**. MS (ESI): m/z ($M + H$)⁺ 392.

5-Morpholino-3-(piperidin-1-yl)-7H-thieno[3,2-*b*]pyran-7-one (17). A 0.5 mL microwave vial was charged with a magnetic stirring bar, compound **6** (50 mg, 158 μmol), cesium carbonate (103 mg, 316 μmol), copper(I) iodide (3 mg, 31 μmol), ethyl 2-oxocyclohexanecarboxylate (10 μL , 63 μmol), and piperidine (200 μL). The reaction mixture was sealed, and the reaction mixture was magnetically stirred and heated via microwave irradiation at 150 °C for 15 min to give desired product **17**. MS (ESI): m/z ($M + H$)⁺ 321.

5-Morpholino-3-(4-morpholinophenyl)-7H-thieno[3,2-*b*]pyran-7-one (18). A 2 mL conical microwave vial was charged with a magnetic stirring bar, compound **42** (80 mg, 230 μmol), sodium *tert*-butoxide (31 mg, 322 μmol), tris(dibenzylideneacetone)dipalladium(0) (3 mg, 3.5 μmol), 2-dicyclohexylphosphino-2',4',6'-triisopropylbiphenyl (8.8 mg, 21 μmol), dimethoxyethane (0.5 mL), and morpholine (24 μL , 276 μmol). The reaction mixture was sealed, and the reaction mixture was magnetically stirred and heated via microwave irradiation at 150 °C for 15 min to give desired product **18**. MS (ESI): m/z ($M + H$)⁺ 399.

2-Morpholino-8-phenyl-4H-chromene-4-thione (20). A 2 mL conical microwave vial was charged with a magnetic stirring bar, 2-morpholino-8-phenyl-4H-chromen-4-one (**1**) (150 mg, 488 μmol), Lawesson's reagent (118 mg, 293 μmol), and toluene (2 mL). The reaction mixture was sealed, and the reaction mixture was magnetically stirred and heated via microwave irradiation at 130 °C for 20 min. The final mixture was poured onto water (approximately 30 mL), extracted with dichloromethane (3 \times 5 mL), the combined extracts dried over anhydrous magnesium sulfate, filtered, and concentrated to dryness. Purification via column chromatography (silica gel; hexanes/ethyl acetate (1:1), then 100% ethyl acetate) afforded pure thione **20** (128 mg, 81% yield). ^1H NMR (DMSO- d_6): 8.50 (dd, J = 8.0, 1.7 Hz, 1H), 7.69–7.45 (m, 7H), 6.90 (s, 1H), 3.67 (t, J = 4.9 Hz, 4H), 3.50 (t, J = 4.9 Hz, 4H). MS (ESI): m/z ($M + H$)⁺ 324.

3-(2,3-Dihydrobenzo[*b*][1,4]dioxin-6-yl)-5-morpholino-7H-thieno[3,2-*b*]pyran-7-thione (21). Compound **21** was prepared from compound **43** under the same reaction conditions described for compound **20**. ^1H NMR (DMSO- d_6): 8.07 (s, 1H), 7.22–7.19 (m, 2H), 6.98 (dd, J = 8.0, 0.8 Hz, 1H), 5.53 (s, 1H), 4.28 (s, 4H), 3.71 (t, J = 5.0 Hz, 4H), 3.43 (t, J = 4.9 Hz, 4H). MS (ESI): m/z ($M + H$)⁺ 388.

1-(2-Hydroxybiphenyl-3-yl)-3-(tetrahydro-2H-pyran-4-yl)propane-1,3-dione (24). An oven-dried 100 mL round-bottom flask was charged with a magnetic stirring bar, tetrahydrofuran (10 mL), and lithium diisopropylamide (2.0 M in hexanes, 6.9 mL, 13.8 mmol). The mixture was magnetically stirred and cooled to 0 °C under argon gas. 1-(2-Hydroxybiphenyl-3-yl)ethanone (0.92 g, 4.34 mmol) was added, and the reaction was stirred at 0 °C for 1 h. A solution of methyl tetrahydro-2H-pyran-4-carboxylate (1.0 g, 6.94 mmol) in tetrahydrofuran (2 mL) was added dropwise over 5 min, and the reaction was allowed to warm to room temperature overnight. The reaction was quenched by the addition of aqueous 10% hydrochloric acid solution (20 mL) until pH = 3. The resulting solution was transferred to a separatory funnel, diluted with water (80 mL), and extracted three times with dichloromethane (100 mL). The organic layers were combined, dried over magnesium sulfate, filtered, and concentrated in vacuo to give crude 1-(2-hydroxybiphenyl-3-yl)-3-(tetrahydro-2H-pyran-4-yl)propane-1,3-dione as a brown oil. The crude product was used as is without further purification.

8-Phenyl-2-(tetrahydro-2H-pyran-4-yl)-4H-chromen-4-one (25). A 5 mL microwave vial was charged with a magnetic stirring bar, crude **24** (320 mg, 1 mmol), ethanol (3 mL), and copper(II) chloride (13 mg, 0.1 mmol). The reaction vial was sealed, the reaction mixture magnetically stirred and heated via microwave irradiation at 140 °C for 10 min. The resulting solution was concentrated in vacuo and purified by high-pressure liquid chromatography to give desired product **25**. ¹H NMR (CD₃OD): 8.12 (dd, *J* = 8.1, 1.6 Hz, 1H), 7.78 (dd, *J* = 7.5, 1.6 Hz, 1H), 7.64–7.40 (m, 6H), 6.29 (s, 1H), 3.97 (dd, *J* = 11.4, 2.6 Hz, 2H), 3.48 (dt, *J* = 11.6, 2.3 Hz, 2H), 2.89 (tt, *J* = 11.5, 4.0 Hz, 1H), 1.89–1.63 (m, 4H). MS (ESI): *m/z* (*M* + *H*)⁺ 307.

5-Morpholino-3-phenyl-7H-thieno[3,2-*b*]pyran-7-one (26). A 2 mL conical microwave vial was charged with a magnetic stirring bar, 3-bromo-5-morpholino-7H-thieno[3,2-*b*]pyran-7-one (**6**) (50 mg, 0.16 mmol), phenylboronic acid (29 mg, 0.24 mmol), cesium carbonate (103 mg, 0.32 mmol), tetrakis(triphenylphosphine)palladium(0) (9 mg, 0.008 mmol), and dimethoxyethane (1 mL). The reaction mixture was magnetically stirred and heated via microwave irradiation for 15 min at 130 °C. Upon cooling to room temperature, the reaction was concentrated in vacuo and purified using high-pressure liquid chromatography to give 5-morpholino-3-phenyl-7H-thieno[3,2-*b*]pyran-7-one (**26**) (10 mg, 3.2 μmol) as a white solid. ¹H NMR (DMSO-*d*₆): 8.18 (s, 1H), 7.72 (dd, *J* = 8.5, 1.3 Hz, 2H), 7.51 (dd, *J* = 8.1, 7.0 Hz, 2H), 7.42 (d, *J* = 7.4 Hz, 1H), 5.54 (s, 1H), 3.71 (t, *J* = 5.0 Hz, 4H), 3.43 (t, *J* = 4.9 Hz, 4H). MS (ESI): *m/z* (*M* + *H*)⁺ 314.

5-Morpholino-3-(pyridin-3-yl)-7H-thieno[3,2-*b*]pyran-7-one (27). A 2 mL conical microwave vial was charged with a magnetic stirring bar, 3-bromo-5-morpholino-7H-thieno[3,2-*b*]pyran-7-one (**6**) (50 mg, 0.16 mmol), 3-pyridylboronic acid (29 mg, 0.24 mmol), cesium carbonate (103 mg, 0.32 mmol), dichloro[1,1'-bis-(diphenylphosphino)ferrocene]palladium(II) dichloromethane adduct (9 mg, 0.008 mmol), and dimethoxyethane (1 mL). The reaction mixture was magnetically stirred and heated via microwave irradiation for 15 min at 180 °C. Upon cooling to room temperature, the reaction was concentrated in vacuo and purified using high-pressure liquid chromatography to give 5-morpholino-3-(pyridin-3-yl)-7H-thieno[3,2-*b*]pyran-7-one (**27**) (6 mg, 1.9 μmol) as a white solid. ¹H NMR (DMSO-*d*₆): 8.94 (dd, *J* = 2.3, 0.9 Hz, 1H), 8.61 (dd, *J* = 4.9, 1.6 Hz, 1H), 8.33 (s, 1H), 8.14 (ddd, *J* = 7.8, 2.3, 1.6 Hz, 1H), 7.55 (ddd, *J* = 7.8, 4.9, 0.9 Hz, 1H), 5.56 (s, 1H), 3.71 (t, *J* = 4.9 Hz, 4H), 3.42 (t, *J* = 5.0 Hz, 4H). MS (ESI): *m/z* (*M* + *H*)⁺ 315.

Methyl 3-Hydroxy-4-(5-morpholino-7-oxo-7H-thieno[3,2-*b*]pyran-3-yl)thiophene-2-carboxylate (85). A 2 mL conical microwave vial was charged with a magnetic stirring bar, compound **9** (57 mg, 0.16 mmol), cesium carbonate (102 mg, 0.31 mmol), methyl 4-bromo-3-hydroxythiophene-2-carboxylate (56 mg, 0.24 mmol), tetrakis(triphenylphosphine)palladium(0) (9 mg, 0.08 mmol), and dimethoxyethane (0.5 mL). The reaction mixture was magnetically stirred and heated via microwave irradiation for 15 min at 140 °C. Upon cooling to room temperature, the reaction was concentrated in vacuo and the residue purified via high-pressure liquid chromatog-

raphy to afford desired product (**85**). ¹H NMR (DMSO-*d*₆): 10.20 (s, 1H), 8.14 (t, *J* = 1.8 Hz, 1H), 7.55 (s, 1H), 5.52 (s, 1H), 3.96 (s, 3H), 3.88 (s, 4H), 3.45 (s, 4H). MS (ESI): *m/z* (*M* - *H*)⁻ 392.

5-Morpholino-3-(1H-pyrrol-2-yl)-7H-thieno[3,2-*b*]pyran-7-one (87). A 20 mL vial was charged with a magnetic stirring bar, Boc-protected compound **65** (50 mg, 124 μmol), and hydrochloric acid (4.0 M in dioxane, 10 mL). The reaction mixture was magnetically stirred overnight at room temperature, concentrated in vacuo, and purified via reverse phase high-pressure liquid chromatography to give desired product **87**. ¹H NMR (CDCl₃): 8.96 (s, 1H), 7.55 (s, 1H), 6.93 (s, 1H), 6.53 (s, 1H), 6.33 (s, 1H), 5.48 (s, 1H), 3.85 (s, 4H), 3.49 (s, 4H). MS (ESI): *m/z* (*M* + *H*)⁺ 303.

5-Morpholino-3-(phenylethynyl)-7H-thieno[3,2-*b*]pyran-7-one (88). A microwave vial was charged with a magnetic stirring bar, compound **6** (50 mg, 158.1 μmol), phenylacetylene (32.0 mg, 316.2 μmol), *trans*-dichlorobis(triphenylphosphine)palladium(II) (5.6 mg, 7.9 μmol), copper(I) iodide (1.6 mg, 7.9 μmol), and diisopropylamine (1.0 mL). The mixture was magnetically stirred and heated via microwave irradiation at 100 °C for 20 min. The mixture was cooled to room temperature and then concentrated in vacuo, resulting in a brown solid. The solid was dissolved in methanol (1.0 mL) and loaded onto an Isolute functionalized silica column (PE-AX/SCX-2). The column was washed with methanol and 7N methanolic ammonia. The methanolic ammonia fractions were combined and concentrated in vacuo. The resulting solid was purified using preparative high-pressure liquid chromatography to give desired product **88** (24.0 mg, 71.1 μmol) as an orange solid. ¹H NMR (DMSO-*d*₆): 8.31 (s, 1H), 7.59–7.57 (m, 2H), 7.48–7.44 (m, 3H), 5.53 (s, 1H), 3.74 (t, *J* = 4.9 Hz, 4H), 3.49 (t, *J* = 4.9 Hz, 4H). MS (ESI): *m/z* (*M* + *H*)⁺ 338.

5-Morpholino-7-oxo-*N*-phenyl-7H-thieno[3,2-*b*]pyran-3-carboxamide (97). A 2 mL microwave vial was charged with a magnetic stirring bar, compound **6** (100 mg, 316 μmol), molybdenumhexacarbonyl (42 mg, 160 μmol), *trans*-di(*μ*-acetato)bis[*o*-(di-*o*-tolylphosphino)benzyl]dipalladium(II) (4.6 mg, 4.9 μmol), tri-*tert*-butylphosphonium tetrafluoroborate (2.8 mg, 12.0 μmol), tetrahydrofuran (500 μL), aniline (45 μL, 483 μmol), and 1,8-diazabicyclo[5.4.0]undec-7-ene (32 μL, 210 μmol). The vial was immediately sealed, magnetically stirred, and heated via microwave irradiation at 125 °C for 6 min. The mixture was cooled to room temperature and loaded onto an Isolute functionalized silica column (PE-AX/SCX-2). The column was washed with methanol, and the product was eluted with 7N methanolic ammonia. The methanolic ammonia fractions were combined and concentrated in vacuo. The resulting solid was purified using preparative high-pressure liquid chromatography to give desired product **97** (3.88 mg, 10.9 μmol) as a yellow solid. ¹H NMR (CDCl₃): 8.24 (s, 1H), 8.18 (s, 1H), 7.64–7.20 (m, 5H), 5.46 (s, 1H), 3.82 (s, 4H), 3.46 (s, 4H). MS (ESI): *m/z* (*M* + *H*)⁺ 357.

Phenyl 5-Morpholino-7-oxo-7H-thieno[3,2-*b*]pyran-3-carboxylate (105). A 2 mL conical microwave vial was charged with a magnetic stirring bar, compound **6** (50 mg, 158 μmol), phenol (22 mg, 237 μmol), molybdenum hexacarbonyl (42 mg, 158 μmol), *trans*-di(*μ*-acetato)bis[*o*-(di-*o*-tolylphosphino)benzyl]dipalladium(II) (4 mg, 4.7 μmol), tri-*tert*-butylphosphonium tetrafluoroborate (2.8 mg, 9.5 μmol), tetrahydrofuran (0.5 mL), and 1,8-diazabicyclo[5.4.0]undec-7-ene (71 μL, 474 μmol). The reaction mixture was sealed, and the reaction mixture was magnetically stirred and heated via microwave irradiation at 125 °C for 6 min to give ester **105**. MS (ESI): *m/z* (*M* + *H*)⁺ 358.

5-Morpholino-7-oxo-7H-thieno[3,2-*b*]pyran-3-carboxylic Acid (106). A 2 mL conical microwave vial was charged with a magnetic stirring bar, compound **6** (50 mg, 158 μmol), molybdenum hexacarbonyl (42 mg, 158 μmol), *trans*-di(*μ*-acetato)bis[*o*-(di-*o*-tolylphosphino)benzyl]dipalladium(II) (2.0 mg, 2.3 μmol), tri-*tert*-butylphosphonium tetrafluoroborate (1.4 mg, 4.7 μmol), dimethyl sulfoxide (0.5 mL), water (2.8 μL, 158 μmol), and 1,8-diazabicyclo[5.4.0]undec-7-ene (16 μL, 106 μmol). The reaction mixture was sealed, and the reaction mixture was magnetically stirred and heated via microwave irradiation at 125 °C for 6 min to give the desired carboxylic acid **106**. MS (ESI): *m/z* (*M* - *H*)⁻ 280.

3-Acetyl-5-morpholino-7H-thieno[3,2-b]pyran-7-one (107).

A 2 mL conical microwave vial was charged with a magnetic stirring bar, compound **6** (100 mg, 316 μmol), dimethylformamide (0.5 mL), *N,N*-diisopropylethylamine (165 μL , 949 μmol), butyl vinyl ether (124 μL , 949 μmol), and dichloro[1,1'-bis(diphenylphosphino)ferrocene]-palladium(II) dichloromethane adduct (10 mg, 12.6 μmol). The reaction mixture was sealed, and the reaction mixture was magnetically stirred and heated via microwave irradiation at 180 °C for 15 min. After cooling to room temperature, the reaction was charged with aqueous hydrochloric acid (1.0 M, 2 mL) and stirred at room temperature for 2 h to give desired ketone **107**. MS (ESI): m/z ($M + H$)⁺ 280.

N-Benzyl-4-(5-morpholino-7-oxo-7H-thieno[3,2-b]pyran-3-yl)benzamide (108). A 2 mL conical microwave vial was charged with a magnetic stirring bar, compound **42** (80 mg, 230 μmol), *trans*-di(μ -acetato)bis[*o*-(di-*o*-tolyl-phosphino)benzyl]dipalladium(II) (6 mg, 7 μmol), tri-*tert*-butylphosphonium tetrafluoroborate (4 mg, 14 μmol), molybdenumhexacarbonyl (61 mg, 230 μmol), tetrahydrofuran (500 μL), benzylamine (75 μL , 690 μmol), and 1,8-diazabicyclo[5.4.0]undec-7-ene (103 μL , 690 μmol). The reaction mixture was magnetically stirred and heated via microwave irradiation for 15 min at 170 °C. Upon cooling to room temperature, the reaction was concentrated in vacuo and purified using high-pressure liquid chromatography to give desired product **108** as a white solid. ¹H NMR (DMSO-*d*₆): 9.14 (t, J = 5.7 Hz, 1H), 8.30 (s, 1H), 8.04 (d, J = 6.0 Hz, 2H), 7.84 (d, J = 6.0 Hz, 2H), 7.34 (d, J = 6.0 Hz, 4H), 7.30–7.18 (m, 1H), 5.56 (s, 1H), 4.51 (d, J = 6.5 Hz, 2H), 3.72 (t, J = 4.4 Hz, 4H), 3.45 (s, 4H). MS (ESI): m/z ($M + H$)⁺ 447.

Butyl 3-(5-Morpholino-7-oxo-7H-thieno[3,2-b]pyran-3-yl)benzoate (118). A 2 mL microwave vial was charged with a magnetic stirring bar, compound **61** (80 mg, 230 μmol), imidazole (47 mg, 690 μmol), molybdenum hexacarbonyl (60 mg, 230 μmol), *trans*-di(μ -acetato)bis[*o*-(di-*o*-tolyl-phosphino)benzyl]dipalladium(II) (6.5 mg, 6.9 μmol), tri-*tert*-butylphosphonium tetrafluoroborate (4.0 mg, 13.9 μmol), tetrahydrofuran (500 μL), *n*-butanol (63 μL , 690 μmol), and 1,8-diazabicyclo[5.4.0]undec-7-ene (103 μL , 690 μmol). The vial was immediately sealed, and the reaction mixture was magnetically stirred and heated via microwave irradiation at 170 °C for 15 min in a microwave reactor to give desired butyl ester **118**. MS (ESI): m/z ($M + H$)⁺ 414.

N-(4-(5-Morpholino-7-oxo-7H-thieno[3,2-b]pyran-3-yl)phenyl)nicotinamide (119). A 40 mL vial was charged with a magnetic stirring bar, compound **60** (200 mg, 609 μmol), and pyridine (5 mL). The mixture was magnetically stirred and cooled to 0 °C in an ice bath. Isonicotinoyl chloride hydrochloric acid (669 μmol) was added, and the reaction was stirred at room temperature for 30 min. The reaction was diluted with dichloromethane (15 mL) and washed three times with saturated aqueous sodium bicarbonate solution (15 mL). The dichloromethane layer was dried over magnesium sulfate, filtered, and concentrated in vacuo to give desired product **119** (94 mg, 217 μmol) as a yellow solid. ¹H NMR (CD₃OD): 9.11 (s, 1H), 8.78 (s, 1H), 8.40 (s, 1H), 7.99 (s, 1H), 7.89–7.70 (m, 6H), 5.60 (s, 1H), 3.56 (s, 4H), 3.31 (s, 4H). MS (ESI): m/z ($M + H$)⁺ 434.

Cell-Based Assays. Cell lines were obtained from the American Type Culture Collection (ATCC, Manassas, VA, catalogue no. CRL-1435). Two thousand cells from the cell lines were placed in 50 μL of complete RPMI 1640 media (Invitrogen, Carlsbad, CA, catalogue no. 22400–105) with 10% fetal bovine serum (Invitrogen, Carlsbad, CA, catalogue no. 10438–026) into each well of 96-well cell culture plates in a hexaplicate sampling pattern. A 50 μL aliquot of test compound (prepared from stock test compounds in DMSO diluted into media) was added to the appropriate well such that the final concentrations of test compound were 200, 40, 8, 1.6, 0.32, 0.064, 0.0128, 0.00256, and 0 μM , and the final DMSO concentration was less than or equal to 0.2%. The plates were incubated for 72 h at 37 °C in an atmosphere of 5% CO₂. At the end of this time, a 10 μL aliquot of WST solution (Roche Applied Science, Mannheim, Germany) was added into each of the wells. Cells were exposed to the WST solution for 4 h. A SpectraMax Plus spectrophotometric plate reader (Molecular Devices, Sunnyvale, CA) was then used to measure the optical density at 450 nm (OD450

nm). Sigmoidal curves were drawn for the dose–responses, and IC₅₀ values were calculated using the software package GraphPad Prism4 (GraphPad Software, Inc., San Diego, CA), and from these graphs the concentration required to decrease proliferation by 50% was calculated.

pAKT Status in Prostate Cancer Cells (PC3). PC3 cells were obtained from the American Type Culture Collection (ATCC, Manassas, VA, catalogue no. CRL-1435). Two million cells from the prostate cancer line PC3 were placed into 6 cm culture dishes and allowed to grow in complete RPMI 1640 media (Invitrogen, Carlsbad, CA, catalogue no. 22400–105) with 10% fetal bovine serum (Invitrogen, Carlsbad, CA, catalogue no. 10438–026). After this time period, the cells were serum starved for 5 h, followed by application of the test compound. Test compound was added as a DMSO solution such that the final DMSO concentration in the cell media was less than or equal to 0.2% by volume. After 30 min of exposure, the growth factor stimulant, human IGF-1 (PeproTech, Inc., Rocky Hill, NJ, catalogue no. 100–11), was added to a final concentration of 0.1 $\mu\text{g/mL}$ in each well. After 30 min of IGF-1 exposure, cells were removed from the media and cell lysates were prepared using RIPA Lysis buffer (Upstate, Lake Placid, NY, catalogue no. 20–188) and kept on ice. The pAKT serine 473 level was measured in duplicate samples of the cell lysates using commercially available assays such as the Pathscan Sandwich ELISA kit for Ser473 pAKT (Cell Signaling, Danvers, MA, catalogue no. 7160). A SpectraMax Plus spectrophotometric plate reader (Molecular Devices, Sunnydale, CA) was used to measure the optical density signal for pAKT at 450 nm (OD450 nm). The pAKT OD450 nm readings were normalized by total protein amount in the cell lysates determined by standard methods.

Concentrations of test compounds required to inhibit IGF stimulated pAKT levels to 50% of maximum levels in PC3 cells (termed DM₅₀ for decreased maximum 50%) were calculated by inputting the dose responses in the software package GraphPad Prism4 (GraphPad Software, Inc., San Diego, CA). These values (in μMolar units) are listed in Table 4.

Cancer Stem Cell Assay. A mammosphere cancer stem cell inhibition assay was modified from that described in the literature^{47,48} using a subset of MCF7 breast cancer cells that possess the ability to evade anchorage independent apoptosis and form mammospheres in vitro. Commercially available MCF7 breast cancer cells were cultured in MEM supplemented with 0.01 mg/mL of bovine insulin and 10% FBS at 37 °C in humidified atmosphere (5% CO₂). Floating cells in the 2-day cultures were collected, washed, and resuspended in DMEM-F12 (50:50) supplemented with 0.4% BSA, 5 $\mu\text{g/mL}$ bovine insulin, 20 ng/mL bFGF, and 10 ng/mL EGF. Cells were then passed through a 40 μM sieve to remove any cell clusters and adjusted to a density of 10000 cells/mL. Approximately 500 cells were plated in quadruplicate in a sterile poly-HEMA-treated 96-well plate. Cells were then treated with either control or test solutions consisting of the kinase inhibitors at 1 or 10 μM . The numbers of mammospheres (clusters of cells numbering more than 4 or 5 cells per cluster) were then counted using a microscope after 5–7 days of incubation and 37 °C, 5% CO₂.

Biostatistical Methodology. The evaluation of difference in the biochemical and cell-based assays was determined using Student *t* test. Experiments were repeated three times.

■ ASSOCIATED CONTENT

Supporting Information

Synthetic methods used for analogues **28–84**, **86**, **89–96**, **98–104**, **109–117**, and **120–127**. This material is available free of charge via the Internet at <http://pubs.acs.org>.

■ AUTHOR INFORMATION

Corresponding Author

*For G.A.M.: phone, (520) 626-1895; fax, (520) 626-0794; E-mail, gmorales@bio5.org. For D.L.D.: phone, (858) 534-3355; fax, (858) 822-0022; E-mail: ddurden@ucsd.edu.

Present Address

[†]For G.A.M.: BIOS Institute (Oro Valley), The University of Arizona, 1580 East Hanley Boulevard, Oro Valley, Arizona 85737, United States. For J.R.G.: SignalRx Pharmaceuticals, 12545 El Camino Real, San Diego, California 92130, United States.

Notes

The authors declare no competing financial interest.

■ ABBREVIATIONS USED

PI3K, phosphatidylinositol-3-kinase; PIP2, phosphatidylinositol(4,5)-bisphosphate; PIP3, phosphatidylinositol(3,4,5)-trisphosphate; PTEN, phosphatase and tensin homologue; AKT, protein kinase B; ATP, adenosine triphosphate; SAR, structure–activity relationship; PIK3CA, phosphoinositide-3-kinase, catalytic, α polypeptide; PIM-1, proviral insertion in murine lymphoma 1 kinase; PLK-1, polo-like kinase 1; DNA-PK, DNA-dependent protein kinase; mTOR, mammalian target of rapamycin; LDA, lithium diisopropylamide; THF, tetrahydrofuran; DME, dimethoxyethane; DCM, dichloromethane; RT, room temperature; MW, microwave irradiation; dppf, 1,1'-bis(diphenylphosphino)-ferrocene; dppp, 1,3-bis(diphenylphosphino)propane; Ar, aromatic; DMSO, dimethyl sulfoxide; DIPEA, diisopropylethylamine; DMF, dimethylformamide; DBU, 1,8-diazabicyclo[5.4.0]undec-7-ene; dba, dibenzylideneacetone; XPhos, 2-dicyclohexylphosphino-2',4',6'-triisopropylbiphenyl; EtOH, ethanol; pAKT, phosphorylated AKT; PDB, Protein Data Bank; compd, compound; PBS, phosphate buffered saline; VEGF, vascular endothelial growth factor; Bv8, *Bombina variegata* peptide 8; IGF, insulin-like growth factor; EGFR, epidermal growth factor receptor; μ M, micromolar; nM, nanomolar; IC₅₀, half maximal inhibitory concentration; PK, pharmacokinetics; NMR, nuclear magnetic resonance; UV, ultraviolet; ELSD, evaporative light scattering detector; HPLC, high pressure liquid chromatography; LCMS, liquid chromatography mass spectrometry; TFA, trifluoroacetic acid; mL, milliliter; min, minute; MS, mass spectrometry; MRA, mass rate attenuator; LC, liquid chromatography; ELS, evaporative light scattering; ESI, electrospray ionization; mg, milligram; mmol, millimole; μ mol, micromole; g, gram; μ L, microliter; ELISA, enzyme-linked immunosorbent assay; DM50, decreased maximum 50%; MEM, minimum essential medium; DMEM, Dulbecco's Modified Eagle's Medium; BSA, bovine serum albumin; bFGF, basic fibroblast growth factor; EGF, epidermal growth factor; cmpd, compound

■ REFERENCES

(1) Shuttleworth, S.; Silva, F.; Tomassi, C.; Cecil, A.; Hill, T.; Rogers, H.; Townsend, P. Progress in the design and development of phosphoinositide 3-kinase (PI3K) inhibitors for the treatment of chronic diseases. *Prog. Med. Chem.* **2009**, *48*, 81–131.
(2) Castellino, R. C.; Muh, C. R.; Durden, D. L. PI-3 kinase-PTEN signaling node: an intercept point for the control of angiogenesis. *Curr. Pharm. Des.* **2009**, *15*, 380–388.
(3) Dienstmann, R.; Rodon, J.; Markman, B.; Tabernero, J. Recent developments in anti-cancer agents targeting PI3K, Akt and mTORC1/2. *Recent Pat. Anticancer Drug Discovery* **2011**, *6*, 210–36.

(4) Markman, B.; Dienstmann, R.; Tabernero, J. Targeting the PI3K/Akt/mTOR pathway—beyond rapalogs. *Oncotarget* **2010**, *1*, 530–543.
(5) Jarvis, L. PI3K at the clinical crossroads. *Chem. Eng. News* **2011**, *89*, 15–19.
(6) Pezet, S.; Marchand, F.; D'Mello, R.; Grist, J.; Clark, A. K.; Malcangio, M.; Dickenson, A. H.; Williams, R. J.; McMahon, S. B. Phosphatidylinositol 3-kinase is a key mediator of central sensitization in painful inflammatory conditions. *J. Neurosci.* **2008**, *28*, 4261–4270.
(7) Ihle, N. T.; Williams, R.; Chow, S.; Chew, W.; Berggren, M. I.; Paine-Murrieta, G.; Minion, D. J.; Halter, R. J.; Wipf, P.; Abraham, R.; Kirkpatrick, L.; Powis, G. Molecular pharmacology and antitumor activity of PX-866, a novel inhibitor of phosphoinositide-3-kinase signaling. *Mol. Cancer Ther.* **2004**, *3*, 763–772.
(8) Vlahos, C. J.; Matter, W. F.; Hui, K. Y.; Brown, R. F. A specific inhibitor of phosphatidylinositol 3-kinase, 2-(4-morpholinyl)-8-phenyl-4H-1-benzopyran-4-one (LY294002). *J. Biol. Chem.* **1994**, *269*, 5241–5248.
(9) Walker, E. H.; Pacold, M. E.; Perisic, O.; Stephens, L.; Hawkins, P. T.; Wymann, M. P.; Williams, R. L. Structural determinants of phosphoinositide 3-kinase inhibition by wortmannin, LY294002, quercetin, myricetin, and staurosporine. *Mol. Cell* **2000**, *6*, 909–919.
(10) Maira, S. M.; Furet, P.; Stauffer, F. Discovery of novel anticancer therapeutics targeting the PI3K/Akt/mTOR pathway. *Future Med. Chem.* **2009**, *1*, 137–155.
(11) Knight, Z. A.; Shokat, K. M. Chemically targeting the PI3K family. *Biochem. Soc. Trans.* **2007**, *35*, 245–249.
(12) Garlich, J. R.; De, P.; Dey, N.; Su, J. D.; Peng, X.; Miller, A.; Murali, R.; Lu, Y.; Mills, G. B.; Kundra, V.; Shu, H. K.; Peng, Q.; Durden, D. L. A vascular targeted pan phosphoinositide 3-kinase inhibitor prodrug, SF1126, with antitumor and antiangiogenic activity. *Cancer Res.* **2008**, *68*, 206–215.
(13) Foukas, L. C.; Berenjeno, I. M.; Gray, A.; Khwaja, A.; Vanhaesebroeck, B. Activity of any class IA PI3K isoform can sustain cell proliferation and survival. *Proc. Natl. Acad. Sci. U. S. A.* **2010**, *107*, 11381–11386.
(14) Edling, C. E.; Selvaggi, F.; Buus, R.; Maffucci, T.; Di Sebastiano, P.; Friess, H.; Innocenti, P.; Kocher, H. M.; Falasca, M. Key role of phosphoinositide 3-kinase class IB in pancreatic cancer. *Clin. Cancer Res.* **2010**, *16*, 4928–4937.
(15) Fruman, D. A.; Rommel, C. PI3Kdelta inhibitors in cancer: rationale and serendipity merge in the clinic. *Cancer Discovery* **2011**, *1*, 562–572.
(16) Jamieson, S.; Flanagan, J. U.; Kolekar, S.; Buchanan, C.; Kendall, J. D.; Lee, W. J.; Rewcastle, G. W.; Denny, W. A.; Singh, R.; Dickson, J.; Baguley, B. C.; Shepherd, P. R. A drug targeting only p110alpha can block phosphoinositide 3-kinase signalling and tumour growth in certain cell types. *Biochem. J.* **2011**, *438*, 53–62.
(17) Brana, I.; Siu, L. L. Clinical development of phosphatidylinositol 3-kinase inhibitors for cancer treatment. *BMC Med.* **2012**, *10*, 161.
(18) Workman, P.; Clarke, P. A.; Raynaud, F. I.; van Montfort, R. L. Drugging the PI3 kinome: from chemical tools to drugs in the clinic. *Cancer Res.* **2010**, *70*, 2146–2157.
(19) Davies, S. P.; Reddy, H.; Caivano, M.; Cohen, P. Specificity and mechanism of action of some commonly used protein kinase inhibitors. *Biochem. J.* **2000**, *351*, 95–105.
(20) Jacobs, M. D.; Black, J.; Futer, O.; Swenson, L.; Hare, B.; Fleming, M.; Saxena, K. Pim-1 ligand-bound structures reveal the mechanism of serine/threonine kinase inhibition by LY294002. *J. Biol. Chem.* **2005**, *280*, 13728–13734.
(21) Rosenzweig, K. E.; Youmell, M. B.; Palayoor, S. T.; Price, B. D. Radiosensitization of human tumor cells by the phosphatidylinositol 3-kinase inhibitors wortmannin and LY294002 correlates with inhibition of DNA-dependent protein kinase and prolonged G2-M delay. *Clin. Cancer Res.* **1997**, *3*, 1149–1156.
(22) Brunn, G. J.; Williams, J.; Sabers, C.; Wiederrecht, G.; Lawrence, J. C., Jr.; Abraham, R. T. Direct inhibition of the signaling functions of the mammalian target of rapamycin by the phosphoinositide 3-kinase inhibitors, wortmannin and LY294002. *EMBO J.* **1996**, *15*, 5256–5267.

- (23) Yuan, J. H.; Feng, Y.; Fisher, R. H.; Maloid, S.; Longo, D. L.; Ferris, D. K. Polo-like kinase 1 inactivation following mitotic DNA damaging treatments is independent of ataxia telangiectasia mutated kinase. *Mol. Cancer Res.* **2004**, *2*, 417–426.
- (24) Kong, D.; Dan, S.; Yamazaki, K.; Yamori, T. Inhibition profiles of phosphatidylinositol 3-kinase inhibitors against PI3K superfamily and human cancer cell line panel JFCR39. *Eur. J. Cancer* **2010**, *46*, 1111–1121.
- (25) Poh, T. W.; Pervaiz, S. LY294002 and LY303511 sensitize tumor cells to drug-induced apoptosis via intracellular hydrogen peroxide production independent of the phosphoinositide 3-kinase-Akt pathway. *Cancer Res.* **2005**, *65*, 6264–6274.
- (26) Imai, Y.; Yoshimori, M.; Fukuda, K.; Yamagishi, H.; Ueda, Y. The PI3K/Akt inhibitor LY294002 reverses BCRP-mediated drug resistance without affecting BCRP translocation. *Oncol. Rep.* **2012**, *27*, 1703–1709.
- (27) Bondar, V. M.; Sweeney-Gotsch, B.; Andreeff, M.; Mills, G. B.; McConkey, D. J. Inhibition of the phosphatidylinositol 3'-kinase-AKT pathway induces apoptosis in pancreatic carcinoma cells in vitro and in vivo. *Mol. Cancer Ther.* **2002**, *1*, 989–997.
- (28) Hu, L.; Hofmann, J.; Lu, Y.; Mills, G. B.; Jaffe, R. B. Inhibition of phosphatidylinositol 3'-kinase increases efficacy of paclitaxel in in vitro and in vivo ovarian cancer models. *Cancer Res.* **2002**, *62*, 1087–1092.
- (29) Mahadevan, D.; Chiorean, E. G.; Harris, W. B.; Von Hoff, D. D.; Stejskal-Barnett, A.; Qi, W.; Anthony, S. P.; Younger, A. E.; Rensvold, D. M.; Cordova, F.; Shelton, C. F.; Becker, M. D.; Garlich, J. R.; Durden, D. L.; Ramanathan, R. K. Phase I pharmacokinetic and pharmacodynamic study of the pan-PI3K/mTORC vascular targeted pro-drug SF1126 in patients with advanced solid tumours and B-cell malignancies. *Eur. J. Cancer* **2012**, *48*, 3319–3327.
- (30) Mahadevan, D.; Chiorean, E. G.; Harris, W. B.; Von Hoff, D. D.; Garlich, J. R.; Ramanathan, R. K. Phase I. Study of the multikinase prodrug SF1126 in solid tumors and B cell malignancies. 47th Annual Meeting of the American Society of Clinical Oncology (ASCO), Chicago, June 3–7, 2011, p 3015.
- (31) Arai, N.; Miyaoku, T.; Teruya, S.; Mori, A. Synthesis of thiophene derivatives via palladium-catalyzed coupling reactions. *Tetrahedron Lett.* **2008**, *49*, 1000–1003.
- (32) Hook, B. B.; Cortizo, L.; Johansson, A. M.; Westlind-Danielsson, A.; Mohell, N.; Hacksell, U. Derivatives of (R)- and (S)-5-fluoro-8-hydroxy-2-(dipropylamino)tetralin: synthesis and interactions with 5-HT_{1A} receptors. *J. Med. Chem.* **1996**, *39*, 4036–4043.
- (33) Liu, Y.; Yu, H.; Mohell, N.; Nordvall, G.; Lewander, T.; Hacksell, U. Derivatives of *cis*-2-amino-8-hydroxy-1-methyltetralin: mixed 5-HT_{1A}-receptor agonists and dopamine D₂-receptor antagonists. *J. Med. Chem.* **1995**, *38*, 150–160.
- (34) Larhed, M.; Hallberg, A. Microwave-Promoted Palladium-Catalyzed Coupling Reactions. *J. Org. Chem.* **1996**, *61*, 9582–9584.
- (35) Han, M.; Zhang, J. Z. Class I phospho-inositide-3-kinases (PI3Ks) isoform-specific inhibition study by the combination of docking and molecular dynamics simulation. *J. Chem. Inf. Model* **2010**, *50*, 136–145.
- (36) Frederick, R.; Denny, W. A. Phosphoinositide-3-kinases (PI3Ks): combined comparative modeling and 3D-QSAR to rationalize the inhibition of p110 α . *J. Chem. Inf. Model* **2008**, *48*, 629–638.
- (37) Lannutti, B. J.; Meadows, S. A.; Herman, S. E.; Kashishian, A.; Steiner, B.; Johnson, A. J.; Byrd, J. C.; Tyner, J. W.; Loriaux, M. M.; Deininger, M.; Druker, B. J.; Puri, K. D.; Ulrich, R. G.; Giese, N. A. CAL-101, a p110 δ selective phosphatidylinositol-3-kinase inhibitor for the treatment of B-cell malignancies, inhibits PI3K signaling and cellular viability. *Blood* **2011**, *117*, 591–594.
- (38) Shojaei, F.; Ferrara, N. Role of the microenvironment in tumor growth and in refractoriness/resistance to anti-angiogenic therapies. *Drug Resist. Updat.* **2008**, *11*, 219–230.
- (39) Shojaei, F.; Ferrara, N. Refractoriness to antivascular endothelial growth factor treatment: role of myeloid cells. *Cancer Res.* **2008**, *68*, 5501–5504.
- (40) Conley, S. J.; Gheordunescu, E.; Kakarala, P.; Newman, B.; Korkaya, H.; Heath, A. N.; Clouthier, S. G.; Wicha, M. S. Antiangiogenic agents increase breast cancer stem cells via the generation of tumor hypoxia. *Proc. Natl. Acad. Sci. U. S. A.* **2012**, *109*, 2784–2789.
- (41) Korkaya, H.; Paulson, A.; Charafe-Jauffret, E.; Ginestier, C.; Brown, M.; Dutcher, J.; Clouthier, S. G.; Wicha, M. S. Regulation of mammary stem/progenitor cells by PTEN/Akt/beta-catenin signaling. *PLoS Biol.* **2009**, *7*, e1000121.
- (42) Schmidt, C. Lapatinib study supports cancer stem cell hypothesis, encourages industry research. *J. Natl. Cancer Inst.* **2008**, *100*, 694–695.
- (43) Maira, S. M.; Stauffer, F.; Brueggen, J.; Furet, P.; Schnell, C.; Fritsch, C.; Brachmann, S.; Chene, P.; De Pover, A.; Schoemaker, K.; Fabbro, D.; Gabriel, D.; Simonen, M.; Murphy, L.; Finan, P.; Sellers, W.; Garcia-Echeverria, C. Identification and characterization of NVP-BEZ235, a new orally available dual phosphatidylinositol 3-kinase/mammalian target of rapamycin inhibitor with potent in vivo antitumor activity. *Mol. Cancer Ther.* **2008**, *7*, 1851–1863.
- (44) Mukherjee, B.; Tomimatsu, N.; Amancherla, K.; Camacho, C. V.; Pichamoorthy, N.; Burma, S. The dual PI3K/mTOR inhibitor NVP-BEZ235 is a potent inhibitor of ATM- and DNA-PKCs-mediated DNA damage responses. *Neoplasia* **2012**, *14*, 34–43.
- (45) Morales, G. A.; Garlich, J. R.; Su, J. D.; Weber, K. T. Novel compound class of designed PI3K pan and isoform-selective inhibitors. 7th International Congress on Targeted Therapies in Cancer, Washington, DC, August 22–24, 2008.
- (46) Morales, G.; Garlich, J.; Newblom, J.; Peng, X.; Su, J.; Weber, K. SFP6: a new compound class of designed pan- and isoform-selective PI3-kinase small molecule inhibitors. AACR Special Conference on Targeting the PI-3 Kinase Pathway in Cancer, Cambridge, MA, November 11–14, 2008.
- (47) Barbone, D.; Yang, T. M.; Morgan, J. R.; Gaudino, G.; Broaddus, V. C. Mammalian target of rapamycin contributes to the acquired apoptotic resistance of human mesothelioma multicellular spheroids. *J. Biol. Chem.* **2008**, *283*, 13021–13030.
- (48) Phillips, T. M.; McBride, W. H.; Pajonk, F. The response of CD24(–/low)/CD44+ breast cancer-initiating cells to radiation. *J. Natl. Cancer Inst.* **2006**, *98*, 1777–1785.